Norsk institutt for luftforskning
Norwegian Institute for Air Research

Monitoring of long-range transported air pollutants in Norway

Annual Report 2022

Wenche Aas, Sabine Eckhardt, Sverre Solberg and Karl Espen Yttri

NILU report 11/2023

NILU report 11/2023 Norwegian Environment Agency M-2554|2023	ISBN: 978-82-425-3122-3 ISSN: 2464-3327	CLASSIFICATION: A – Unclassified (open report)
DATE 28.06.2023	SIGNATURE OF RESPONSIBLE PERSON Aasmund Fahre Vik Deputy Director and CTO (sign.)	NUMBER OF PAGES 42

TITLE	PROJECT LEADER
Monitoring of long-range transported air pollutants in Norway. Annual Report 2022.	Wenche Aas
	NILU PROJECT NO. O-121002 LANGTR/O-113007/O-113008
AUTHOR(S) Wenche Aas, Sabine Eckhardt, Sverre Solberg and Karl Espen Yttri	QUALITY CONTROLLER Kjetil Tørseth
REPORT PREPARED FOR The Norwegian Environment Agency, P.O. Box 5672 Torgarden, N-7485 Trondheim Contact person: Gunnar Skotte	CONTRACT REF. Contract number 21087006/17078061

ABSTRACT

This report presents results from the monitoring of atmospheric composition and deposition of air pollution in 2022, and focuses on main components in air and precipitation, particulate and gaseous phase of inorganic constituents, particulate carbonaceous matter, ground level ozone and particulate matter. The level of pollution in 2022 was generally low though a few high episodes occurred, i.e., one in March with elevated aerosol concentrations and one during July, with high ozone levels.

NORWEGIAN TITLE

Overvåking av langtransportert forurenset luft og nedbør. Atmosfæriske tilførsler 2022.

KEYWORDS

Atmosphere and climate/ Atmosfære og klima/	Aerosols and particles/ Aerosoler og partikler	Ground level ozone/ Bakkenært ozon	Acid rain and eutrophication/ Sur nedbør og overgjødsling

ABSTRACT (in Norwegian)

Denne rapporten omhandler resultater fra overvåkningsprogrammet for langtransportert forurenset luft og nedbør og atmosfæriske tilførsler i 2022. Rapporten presenterer målinger av uorganiske hovedkomponentene i luft og nedbør, partikulært karbonholdig materiale, partikkelmasse og bakkenært ozon. Forurensningsnivået i 2022 var generelt lavt, men med noen høye episoder, det var til eksempel en episode i mars med høye partikkelkonsentrasjoner og en i juli med høye konsentrasjoner av bakkenær ozon.

PUBLICATION TYPE: Digital document (pdf)

COVER PICTURE: Source: NILU

Citation: Aas, W., Eckhardt, S., Solberg, S., Yttri, K.E. (2023). Monitoring of long-range transported air pollutants in Norway. Annual Report 2022. (NILU report 11/2023). Kjeller: NILU.

NILU's ISO Certifications: NS-EN ISO 9001 and NS-EN ISO 14001. NILU's Accreditation: NS-EN ISO/IEC 17025.

Contents

Summary

The monitoring program for long-range transboundary air pollutants, which is presented in this report, includes measurements of inorganic- and organic compounds, particles, and ground-level ozone. The main purpose is to quantify the levels and document any changes in atmospheric input, which is important for evaluating the effect of air pollution on ecosystems, health, materials, and climate. This report provides an overview of the pollution levels at Norwegian background stations in 2022 and compares these with changes over time. The main findings in the report are:

- Several components have a clear South-North gradient strongly influenced by long-range transport (LRT) from the European continent.
- In March it was a 14-day period with high aerosol concentrations in southern Norway, with a weekly $PM_{2.5}$ concentration of 14.6 $\mu g/m^3$ at Birkenes, thus likely exceeding the Air Quality Guidelines of daily concentrations in this period. The chemical composition shows a mixture of sources, and the air mass trajectories show that the polluted air is from central Europe.
- In July, a peak ozone level of 177 $\mu g/m^3$ was measured at Sandve, the highest annual maximum since 2006 and close to EU's information threshold of 180 $\mu g/m^3$. This episode was caused by an extended European heat wave with record-high temperatures.
- There is a clear reduction in observed concentrations for most of the components in the last 20 years, in line with the emission reductions in Europe. There are also decreasing trends from 2010, but with substantial variations between the sites and components.
- WHO published their updated air quality guidelines in 2021. For ozone the new guideline values will be hard to meet with European emission abatement alone and will in practice require emissions reduction even from other continents.

Sammendrag

Overvåkingsprogrammet for langtransporterte luftforurensninger, som presenteres i denne rapporten, omhandler målinger av uorganiske- og organiske forbindelser, partikler og bakkenært ozon. Hovedmålet er å kvantifisere nivåene og dokumentere eventuelle endringer i atmosfærisk tilførsel, noe som er viktig for å kunne evaluere luftforurensningenes effekt på økosystem, helse, materialer og klima. Denne rapporten gir en oversikt over forurensingsnivået på norske bakgrunnsstasjoner i 2022 og sammenligner disse med utvikling over tid. Hovedfunnene i rapporten er:

- De fleste komponentene har en sør-nord gradient. Dette skyldes både nærheten til kontinentet og at en del av forurensningen fra kontinentet avsettes på vei nordover.
- I mars var det en toukers periode med høye aerosolkonsentrasjoner i Sør-Norge, med et ukesmiddel av $PM_{2,5}$ på 14,6 $\mu g/m^3$ på Birkenes. Høyst sannsynlig ble luftkvalitetskriteriet for daglig eksponering av $PM_{2.5}$ overskredet. Den kjemiske sammensetningen viser en blanding av kilder, og luftmassen med forurenset luft er fra Sentral-Europa.
- I juli ble den høyeste timesverdien av ozon på 177 $\mu g/m^3$ målt på Sandve, det høyeste årlige maksimum siden 2006 og nær EUs informasjonsterskel på 180 $\mu g/m^3$. Denne episoden ble forårsaket av en europeisk hetebølge med rekordhøye temperaturer.
- Det er en klar reduksjon i observerte konsentrasjoner for de fleste av komponentene de siste 20 årene, i tråd med utslippsreduksjonene i Europa. Det er også avtagende trender fra 2010, men det er stor variasjon mellom stasjoner og komponenter.
- WHO publiserte oppdaterte retningslinjer for hvilke nivåer av uteluft som anses som trygge for de aller fleste i befolkningen i 2021. For ozon vil de nye retningslinjene være vanskelige å oppfylle med europeiske utslippsreduksjoner alene og i praksis vil det kreve utslippsreduksjoner også fra andre kontinenter.

Monitoring of long-range transported air pollutants in Norway

Annual Report 2022

1 The monitoring programme.

The main objective of the monitoring programme is to quantify the levels of regional air pollution and to document any changes. These observations are important for studies on the influence on ecosystems, human health, materials, and climate change.

The programme started in 1973 with measurements of sulfur and nitrogen compounds and was soon after extended with ozone. The first observations were conducted in Southern Norway. The measurement programme and the monitoring network was then expanded to provide improved information on atmospheric contribution of air pollution for all of Norway. Aerosol particles and carbonaceous aerosol was included in 2000/1 and aerosol size distribution in 2010.

The atmospheric monitoring programme presented in this report includes observations of sulfur- and nitrogen compounds in air and precipitation, levoglucosan, elemental- and organic carbon (EC/OC) in aerosols, ground level ozone, particulate matter (PM_{10} and $PM_{2.5}$). Data from in total 17 sites in the Norwegian rural background environment is presented. Location and basic information regarding the monitoring programme at various sites are illustrated in Figure 1.1, whereas more detailed information of what is measured at each site can be found in Appendix C

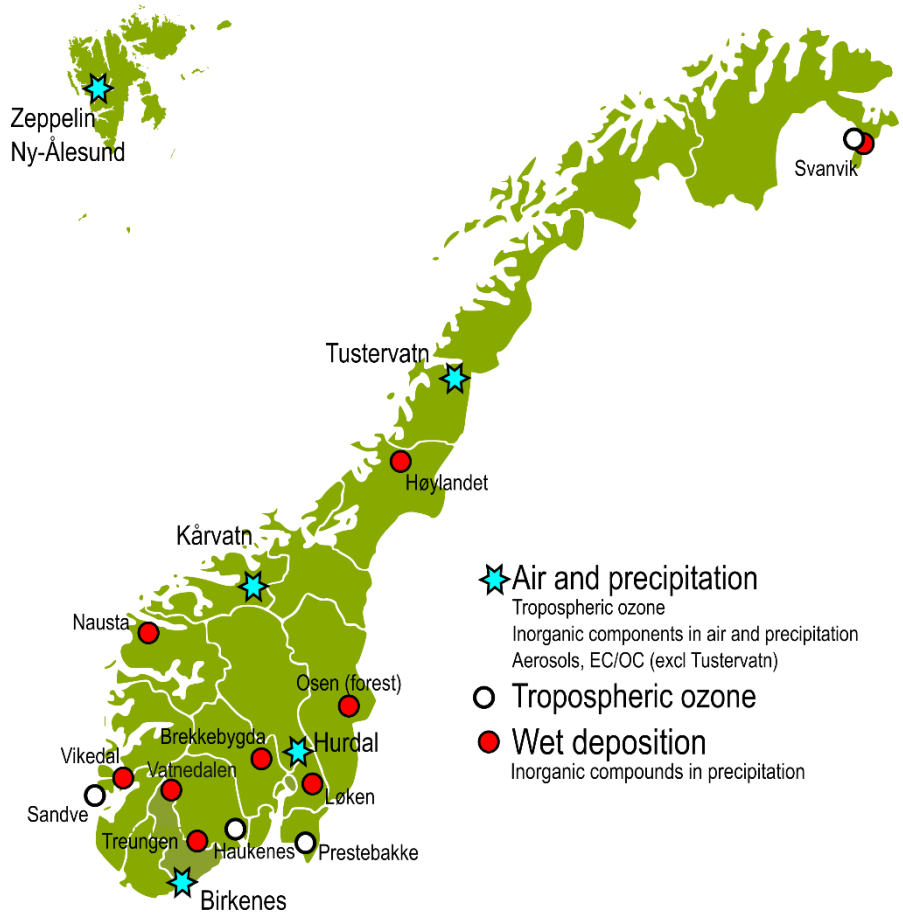

Figure 1.1: Norwegian background sites and their measurement programme 2022.

The national monitoring programme are conducted on behalf of the Norwegian Environment Agency with additional funding from the Ministry of Climate and Environment. The observations in Finnmark county are financed by the Ministry of Foreign Affairs through the Norwegian Environment Agency. The ozone measurements at Haukenes are financed by the local municipalities. Observations from Osen (forest) are part of the national forest damage monitoring conducted by NIBIO (Timmermann et al, 2023)

Data and results from this national monitoring programme are reported to various international programmes and all data are openly available at http://ebas.nilu.no. Details regarding sampling methods and chemical analysis are described in Appendix D .

2 Overview of different Air Quality Guidelines (AQG) and limit values

There is a multitude of target values, limit values and guideline values that sets criteria levels of air pollution to protect health and environment. These are developed by several bodies, i.e.: EU, World Health Organisation (WHO), UN-ECE and by the Norwegian authorities represented by the Norwegian Institute of Public Health and the Norwegian Environmental Agency.

EU has defined limit values for different air pollutants (EU, 2018) and these are implemented in Norwegian law ("Forurensningsforskriften", Chapter 7). Norway has stricter limit values for some components than EU, for instance $PM_{2,5}$ and PM_{10} (FHI,2013). EU also has a set of long-term objectives and target values.

World Health Organisation (WHO) has defined a set of Air Quality Guidelines (AQG) for key air pollutants that pose health risk. WHO published updated AQG in 2021, and for some pollutants the concentrations that can cause health damage are substantially lower than the previous AQG published in 2005 (WHO, 2021). National authorities have published Air quality Criteria, that are based on the AQG from WHO, but also on other relevant research on air pollution and health effects. The air quality criteria for PM and NO_2 were revised in 2023, and the criteria for ozone are expected to be updated in the near future (FHI, 2023).

The EU directive (EU, 2018) is currently under revision and a new directive with revised limit values is expected, possibly containing target values for the year 2030. The revised directive will probably be more closely linked to WHO's updated AQG (WHO, 2021).

UN-ECE has developed threshold values for ozone for the protection of vegetation.

An overview of different limit values, targets and guidelines are given for PM in Table 2.1 and for ozone in Table 2.2 (for health) and Table 2.3 (vegetation). Guidelines and limit values for NO_2 and SO_2 are not included since these are not very relevant for Norwegian regional air quality levels.

Table 2.1: EU and national limit values and Air-Quality Guidelines and Criteria for PM_{10} and $PM_{2.5}$.

	24-hours	Annual
EU limit values (EU, 2008)		
PM_{10}	50 µg/m³ (≤ 35 days yr^{-1})	40 µg/m³
$PM_{2.5}$		25 µg/m³
National limit values (FHI 2013)		
PM_{10}	50 µg/m³ (≤ 25 days yr^{-1})	20 µg/m³
$PM_{2.5}$		10 µg/m³
WHO Air-Quality Guidelines (WHO, 2021)		
PM_{10}	45 µg/m³ (the 99th percentile)	15 µg/m³
$PM_{2.5}$	15 µg/m³ (the 99th percentile)	5 µg/m³
National Air-Quality Criteria (FHI 2023)		
PM_{10}	30 µg/m³	15 µg/m³
$PM_{2.5}$	15 µg/m³	5 µg/m³

Table 2.2. Limit values and Air-Quality Guidelines and Criteria for ground-level ozone, for the protection of human health.

Value ($\mu g/m^3$)	Averaging time (hours)	Ref	Description
180	1	EU (2008)	EU's information threshold
240	1	EU (2008)	EU's alert threshold
120	8[1)]	EU (2008)	EU's target value. 8-hour mean value not to be exceeded on more than 25 days per year averaged over 3 years.
120	8[1)]	EU (2008)	EU's long-term objective.
60	8[2)]	WHO (2021)	Mean over the peak season
100	1	FHI (2013)	National Air Quality Criteria
80	8[1]	FHI (2013)	National Air Quality Criteria

1) The highest 8-hour running mean value for each day calculated such that the 8-hour periods are assigned to the day on which the period ends.

2) Defined as the average of the daily maximum 8h running mean concentration in the six consecutive months with the highest 6-months running O_3 concentration.

Table 2.3: Critical levels and target values defined for the protection of vegetation from ozone exposure.

AOT40 (ppb hours)	Period	Reference	Comment
3000	3-months growing season	Mills et al., 2017	UN-ECE's critical level for agricultural crops and semi-natural vegetation [1)]
5000	1 April – 30 Sept	Karlsson et al., 2003; 2005	UN-ECE's critical level for forests [1)]
9000	1 May – 31 July	EU, 2008	EU's target value for vegetation. Should be averaged over five years [2)]
3000	1 May – 31 July	EU, 2008	EU's long-term objective for vegetation [2)]

1) UN-ECE's AOT values should be based on the hours with global incoming radiation > 50 W/m^2
2) EU's AOT values should be based on the period 08-20 CET

3 Status of the observations in 2022

3.1 Annual levels and spatial gradients

Norway is influenced by major anthropogenic emission regions in Europe, being of great importance for the observed levels of air pollutants and their regional distribution. The annual and monthly mean concentration in air and precipitation in 2022 for all sites and components are given in Appendix A.

Several components have a clear South to North gradient strongly influenced by long-range transport (LRT) from the European continent. Figure 3.1 illustrates spatial gradients for selected pollutants in 2022. Sulfate concentrations were highest in south and southeast, except at Svanvik, which is influenced by emissions from Russia with elevated concentrations of especially sulfate. The concentration levels have decreased considerably after the smelter in Nikel closed down in December 2020 (Berglen et al., 2022), though. Wet depositions were highest in southwest, partly due to the high precipitation amount on the west coast. Maximum ozone concentrations showed a similar pattern as for sulfate with highest levels in southern Norway (Figure 3.1).

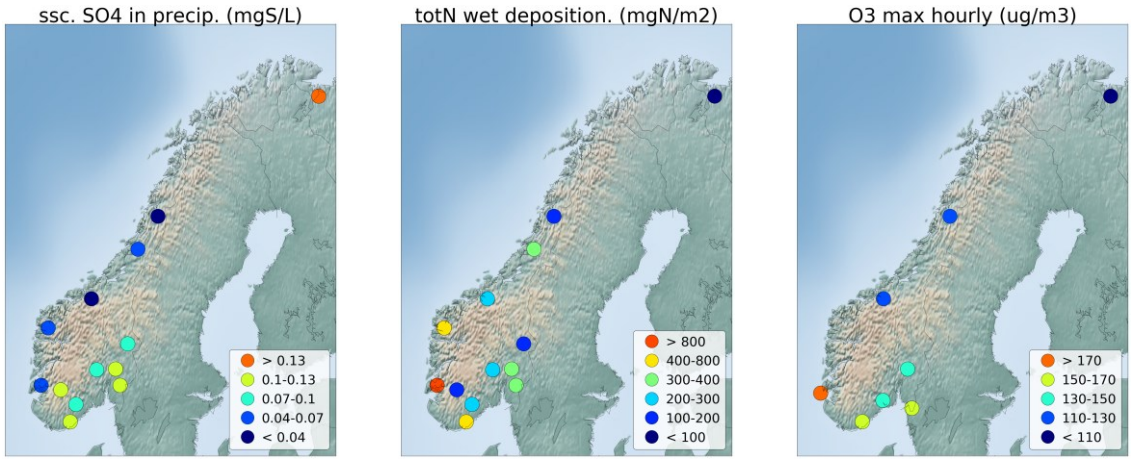

Figure 3.1: Annual volume weighted mean concentrations of sea salt corrected (ssc) sulfate (left), total wet deposition of nitrogen (middle), and the highest hourly concentration of ozone (right) observed in 2022. Note that the colours only represent the spatial distribution and do not indicate any exceedances of limit values or similar.

The air pollution level at Norwegian rural background sites is generally amongst the lowest in Europe (EMEP, 2022). The annual mean aerosol mass concentration in 2022 ranged from 2.6 to 4.3 µg/m^3 (PM_{10}) and 1.2 to 2.4 µg/m^3 ($PM_{2.5}$), causing no violation of national limit values nor exceedances of air quality guidelines (AQG) from WHO (Table 2.1). Carbonaceous aerosol levels (organic carbon (OC) < 1.1 µg C/m^3 and elemental carbon (EC) < 0.09 µg C/m^3) are also relatively low, but up to 7 times higher compared to the remote Arctic environment (OC < 0.15 µg C/m^3 and EC < 0.015 µg C/m^{-3}) (Table A.4).

There were two significant long-range transport (LRT) air pollution episodes observed in 2022: One in March, bringing polluted air masses from Eastern Europe causing elevated aerosol levels (Chapter 3.2), and one in July during a heat wave in Europe, bringing high ozone levels to Norway from Southern and Central Europe (Chapter 3.3).

3.2 Episodes of high concentrations of PM

Long-range atmospheric transport is decisive both for mean and peak levels of particulate matter (PM) in the Norwegian background environment due to low background levels, and both anthropogenic and natural sources are decisive for observed seasonality of PM. Exemplified for carbonaceous aerosol, anthropogenic sources (fossil fuel and residential wood combustion) dominate in winter, whereas natural sources (biogenic secondary organic aerosol (BSOA) and primary biological aerosol particles (PBAP)), dominate the organic aerosol in summer (Yttri et al., 2021). A similar pattern is observed in the remote Arctic, where accumulation of anthropogenic emissions from Eurasia in winter and spring form Arctic haze (Platt et al., 2022; Yttri et al., 2023 subm.). Increased levels of OC in summer relies on occasional LRT episodes with emissions from Boreal Forest fires, which also bring BSOA and PBAP, given the scarce vegetation in the high Arctic.

The energy prices in Europe peaked in 2022 (Eurostat, 2023), which might indicate a shift towards biomass burning for residential heating, as previously seen during economic downturn in Europe (Saffari et al., 2013). However, there was no increase in the level of the biomass burning tracer levoglucosan at Birkenes in 2022 heating season compared to previous years. Notably, the ambient temperature in Continental Europe, being the source region of levoglucosan observed at Birkenes, was higher compared to the long-term mean for a large part of the 2022 heating season and might have alleviated the need for residential heating somewhat. It is estimated that emission from residential wood burning contributed 9% to PM_{10} and 16% to $PM_{2.5}$ in the heating season (October - April) at Birkenes in 2022.

During March, PM levels were elevated for a period of 14 days, causing a weekly mean as high as 20.8 µg m^{-3} of PM_{10} at Birkenes, contributing substantially to the elevated monthly mean of 9.8 µg m^{-3}. The corresponding weekly $PM_{2.5}$ concentration was 14.6 µg m^{-3}. Hence, it cannot be excluded that daily concentrations exceeded 15 µg m^{-3} during this week, exceeding national air quality criteria and WHO AQG. The chemical composition shows a mixture of sources with secondary inorganic aerosol (SIA) (here: sum of SO_4^{2-}, NO_3^-, and NH_4^+) dominating, followed by organic matter (OM = OC × 1.7) and sea salt aerosol (SSA) Hurdal was also influenced by this episode, although not to the same extent.

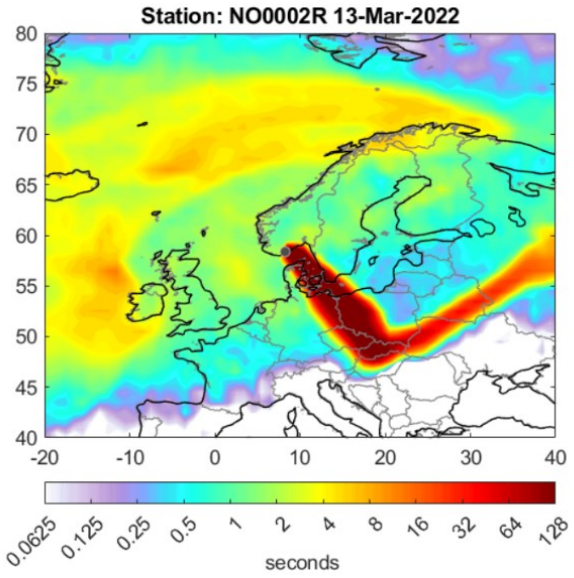

Figure 3.2: Flexpart footprints of the airmasses arriving Birkenes 13 March 2022, calculated with the Flexpart model (Pisso et al., 2019.) The unit (second) shows the residence time in the surface layer (100 m) of the air masses arriving at the actual date at Birkenes

3.3 Episodes of high concentrations of ozone

In summer, episodes of elevated ozone in Norway may occur and these are often associated with a high pressure located over the European continent, typically over Central or Eastern parts, setting up a southerly or south-westerly transport of warm, polluted air masses. Ozone episodes are typically a fair-weather phenomenon associated with hot and sunny days. The northern hemispheric ozone baseline level varies between 40 and 80 μg/m^3 and is typically highest in spring. On top of this baseline level, episodes with long-range transport of more polluted air masses increase the ozone levels regularly in summer. The ozone levels at Norwegian monitoring sites are also influenced by local effects such as surface dry deposition and episodes of local NOx emissions reducing ozone but in general surface ozone in Norway is the result of polluted air masses transported from Europe on top of the hemispheric baseline.

In July it was an extensive ozone episode seen at many sites in Europe (Figure 3.3). This was linked to an extended European heat wave with record-high temperatures and wildfires. On 15 July the Met Office in the UK declared a national emergency, and on 19 July soaring temperatures exceeding 40 °C was recorded in the UK, the highest temperature ever seen in that country.

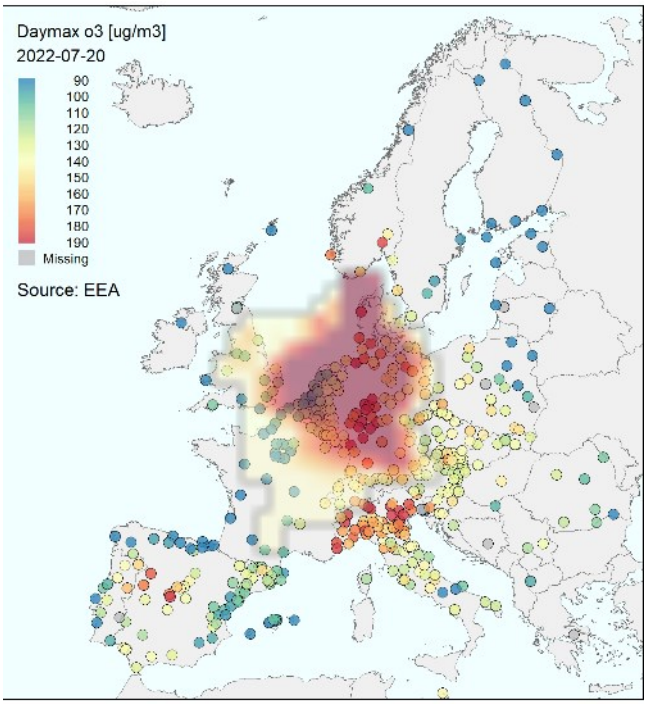

Figure 3.3: Flexpart footprints of the airmasses arriving Birkenes of the airmasses arriving Birkenes 20 July (right), calculated with the Flexpart model (Pisso et al., 2019.) The unit (second) shows the residence time in the surface layer (100 m) of the air masses arriving at the actual date at Birkenes. The figure also includes the daily maximum ozone concentration at European stations the same day as reported to EEA.

Very high temperatures were experienced also in Norway as a fringe of the heat wave touched southern parts of the country and a peak ozone level of 177 ug/m^3 was measured at Sandve (Figure 3.4), the highest annual maximum since 2006 and close to EU's information threshold of 180 ug/m^3.

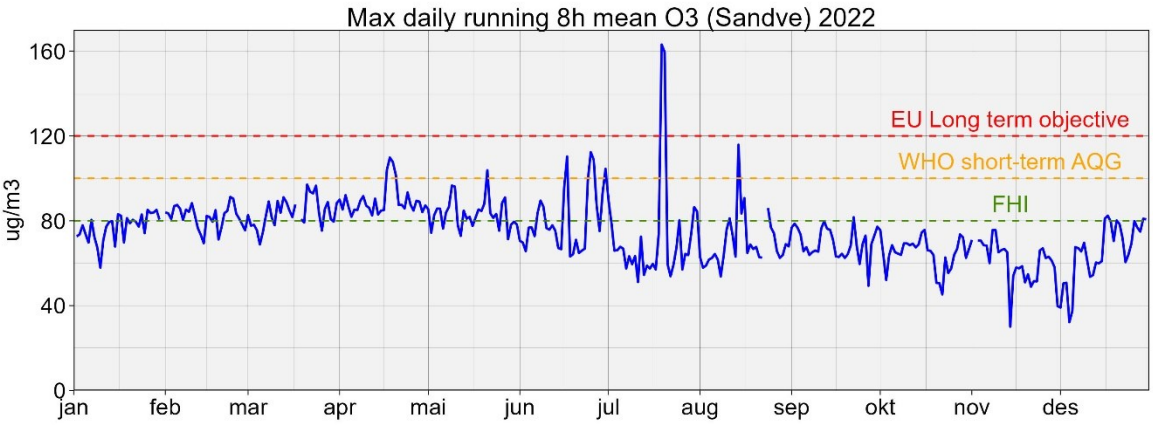

Figure 3.4: Max daily running 8 h (MDA8) at Sandve in 2022 compared to threshold and target values set by EU (2008), WHO (2021) and National authorities (FHI, (2013).

Though this peak exceeded both the EU long-term objective which is implemented in Norwegian legislation (120 μg/m^3), the WHO 8-h AQG (100 μg/m^3) and the Norwegian air quality criteria (80 μg/m^3, see Table 2.2. Several of the other sites also peak in July, see their plots in Figure A.1 and the maximum hourly concentration at all these sites during 2023 in Table A.19.

This episode illustrates very clearly the tight links between climate and surface ozone and is a reason for concern due to the expected increase in climate change in future years.

The very strict AQG set by WHO refers to the so-called peak-season average, implying taking the average over 6 months of the daily maximum 8-h concentration. It is very likely that it will not be possible to meet WHO's AQG with European emission reductions alone since the AQG is close to the baseline level and thus requires emission reductions in other continents as well.

3.4 European measurement campaign of VOCs

During the heat wave describe in Chapter 3.3, a European measurement campaign was conducted to study the ozone distribution as well as the role of precursor gases (VOCs and NOx) during such an episode. The campaign was partly supported by the European Solvents Industry Group (ESIG) and the Norwegian Environment Agency and coordinated by the EMEP Task Force of Measurement and Modelling (TFMM).

A meteorological team studied the weather situation and the forecasts in the summer season prior to the episode and when this strong episode was evident from the forecasts the campaign was initiated and a large number of samplers and other equipment was shipped to labs and institutions all over Europe. The measurement campaign was set between 12-19 July. It turned out that the episode was very well predicted by the forecasts and a unique dataset for surface ozone and hundreds of various VOCs were measured on a pan-European basis during the episode.

The analysis and interpretation of this dataset is challenging and will require time but is expected to result in several scientific papers. Such a campaign covering all of Europe with a widespread range of precursor gases has not been conducted previously. An overview of different monoterpenes measured at Birkenes during this campaign can be seen in Figure 3.5.

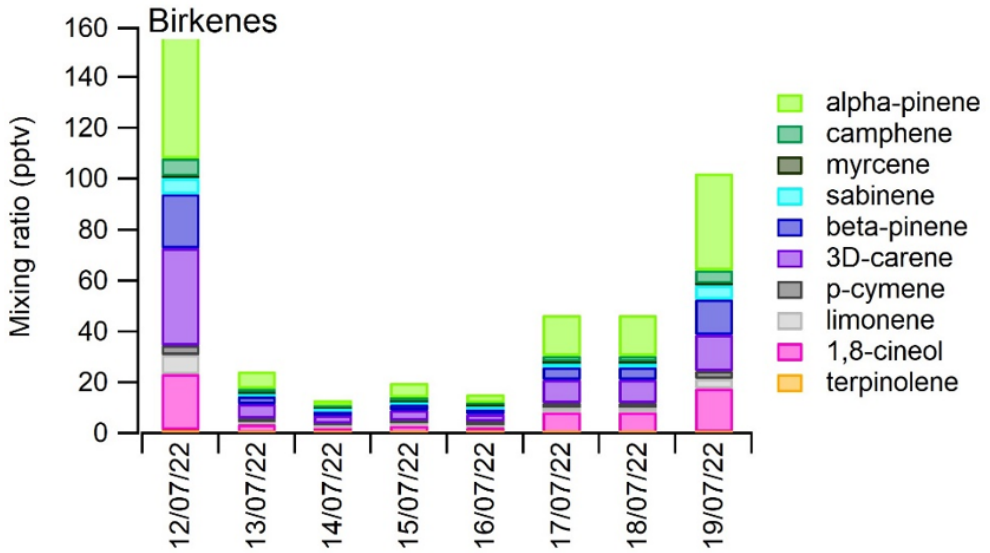

Figure 3.5: Daily variation of monoterpenes during the EMEP intensive measurement period in summer 2022 measured with Tenax tubes analysed at the Finnish Meteorological Institute (figure from Hellen, 2023).

4 Trends in air pollution

An important goal of the monitoring programme is to measure the effectiveness of the protocols, i.e., the 1999 Gothenburg Protocol to Abate Acidification, Eutrophication and Ground-level Ozone (UN/ECE, 1999). Since Norway is influenced by major emission sources in Continental Europe, the Norwegian rural background monitoring network can indicate changes to overall emission reductions in Europe.

For the statistical analysis, the non-parametric Mann-Kendall Test was applied on annual means for detecting and estimating trends (Gilbert, 1987). The Sen-Theil slope estimator was used to quantify the magnitude of the trends (Hussain et al. 2019). Tables with the calculated linear trends for 2000-2022 and 2010-2022 averaged for all sites with measurements in these respective periods are given in Appendix B. For timeseries prior to 2000 it is referred to earlier publications (Aas et al., 2022 and Tørseth et al., 2012).

4.1 Trends in inorganic compounds

Figure 4.1 shows the time series of annual mean concentrations of sulfur and nitrogen components in air and precipitation at selected sites in Norway with long time series. The average trends in sulfur are between -2.7 - -3.3 % per year between 2000-2022 depending on component (Table B.1). There is also a clear reduction in oxidised nitrogen, between -1.5 - -2.4% per year (Table B.1). This is also the case for reduced nitrogen though ammonium in aerosol has a larger reduction (-2.6 %/y) than in precipitation (-0.8 %/y). These large differences between the changes found for the different reduced nitrogen components can be explained by the interaction of ammonia with the sulfur and oxidized nitrogen components. It can be noted that the results imply that the contribution of ammonia emissions to aerosols has been largely reduced during the 2000–2022 period, due to the impact of Sox and NOx emission reductions in Europe (EMEP, 2021). The observed reductions in levels of sulfur and nitrogen species agree with reported downwards trends in pollutant emissions in Europe (Colette et al., 2021; EMEP, 2021, Lewis et al., 2023).

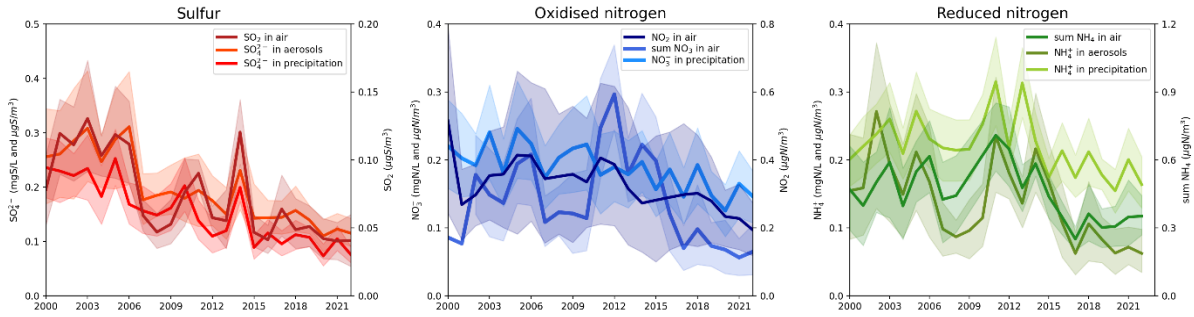

Figure 4.1: Average trends in sulfur and nitrogen components measured at Norwegian background sites (2000-2022). The solid line in the trend plots indicate the average annual mean concentrations for all the sites and the shaded area the 95% confidence interval. There are 11 sites with long term observations of sulfur and nitrogen in precipitation and 5 with measurements in air and aerosol (4 for NO_2).

4.2 Trends in aerosols

Trends in PM measurements are shown in Figure 4.2. More than two decades of PM measurements at Birkenes show a statistically significant decrease both in PM_{10} (-1.7 % yr^{-1}) and $PM_{2.5}$ (-2.5 % yr^{-1}) (2000/1 to 2022) being less pronounced for PM_{10} due to influence from natural sources such as sea salt aerosol (SSA), mineral dust (MD) and primary biological aerosol particles (PBAP), prevailing in the

coarse fraction of PM_{10}. Decreasing levels of SO_4^{2-} and fine fraction organic carbon (OC) contribute most to the reduction in PM, reflecting efficient abatement of anthropogenic SO_2 emissions and OC (and elemental carbon (EC)) from combustion sources. Notably, abatement of OC and EC from fossil fuel combustion appears somewhat more efficient than from biomass burning, considering the lower reduction observed for levoglucosan (-2.5 % yr^{-1}) than for EC (-3.2 % yr^{-1}) (2011 – 2022). PM levels at Hurdal (PM_{10}: -1.2% yr^{-1}; $PM_{2.5}$: -3.0% yr^{-1}) and Kårvatn (PM_{10} -2.1 % yr^{-1}; $PM_{2.5}$: -3.6 % yr^{-1}) decrease at slightly lower rates compared to Birkenes considering identical periods (2011 – 2022), but the decrease is not statistically significant. The reduction is associated with secondary inorganic aerosol (SIA) constituents, primarily NO_3^-.

The SSA concentration at Birkenes has increased over the last two decades (2.6 % yr^{-1}), constituting an equally large fraction (30%) of PM_{10} in 2022 as SIA species (SO_4^{2-}+NO_3^-+NH_4^+) and organic matter (OM), whereas MD accounted for 10% (Figure 4.2). Further, the OC fraction of PM is increasing despite that emission from combustion are declining, emphasizing the importance of organic aerosol from natural sources, being BSOA and PBAP. This shift in aerosol composition at Birkenes reflects a change in the relative source composition of PM. The chemical composition at Hurdal and Kårvatn shows less influence by SIA and SSA, emphasizing the longer distance from important source regions of SIA precursors in continental Europe and to the coast, respectively, with OM (42 – 45%) as the major fraction.

A statistically significant downward trend was observed for EC (-3.1% yr^{-1} to -4.2% yr^{-1}) at all rural background sites, whereas for OC the downward trend was statistically significant only for Birkenes (-1.2 to -1.5%) (Table B.3).

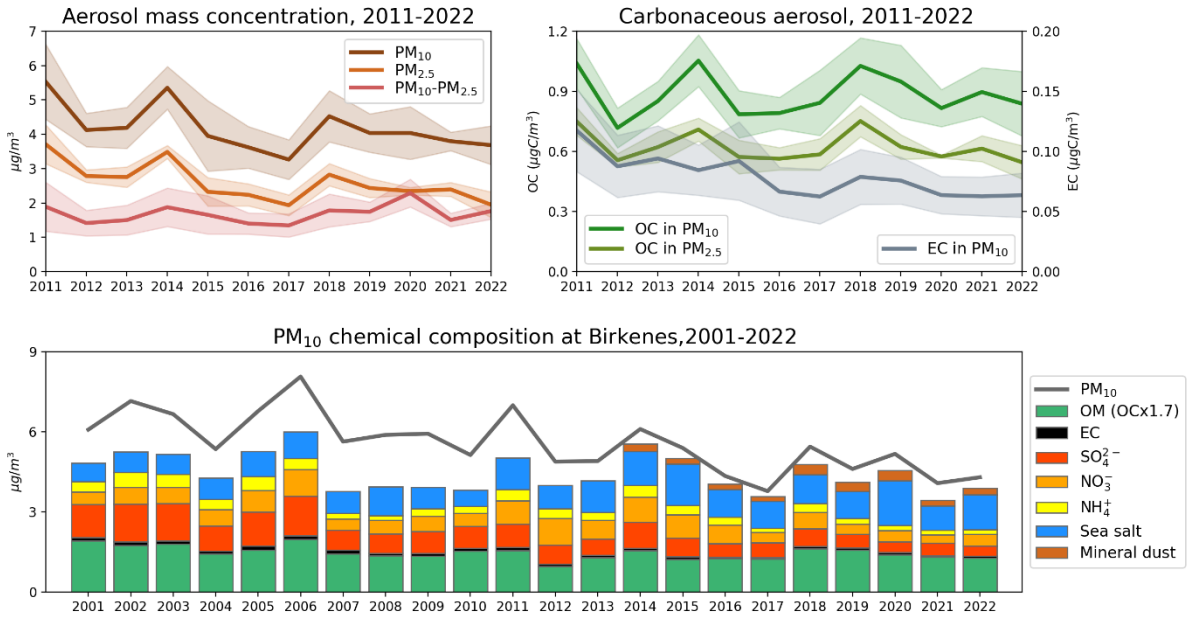

Figure 4.2: Trends for PM_{10}, $PM_{2.5}$, $PM_{10-2.5}$ (upper left) and Carbonaceous aerosol (OC and EC) (upper right) averaged for Birkenes Observatory, Hurdal and Kårvatn (2011 – 2022). Mass closure for PM_{10} at Birkenes (lower panel) (2001 - 2022).

4.3 Trends in surface ozone

For surface ozone, the annual mean concentration has little scientific interest since pollution episodes typically lead to enhanced ozone in summer and reduced levels in winter and thus the impact on the annual mean is unclear. Furthermore, the number and levels of European summer episodes vary from year to year and is closely related to the weather situation. There has, however, been a gradual decrease in the European peak levels since the early 2000s which is reflected also at Norwegian sites. The trends and significance of these are not clear cut though since the peaks are strongly tied to the weather anomalies in the respective years.

Figure 4.3 shows the development of ozone metrics linked to damage on vegetation (AOT40 = Accumulated Ozone over the Threshold of 40 ppb) and human health (number of days with ozone exceeding certain recommendations set by WHO). These time series are characterized by a slow reduction with time while at the same time strongly variable from year to year. The values for human health were particularly low in 2000, though.

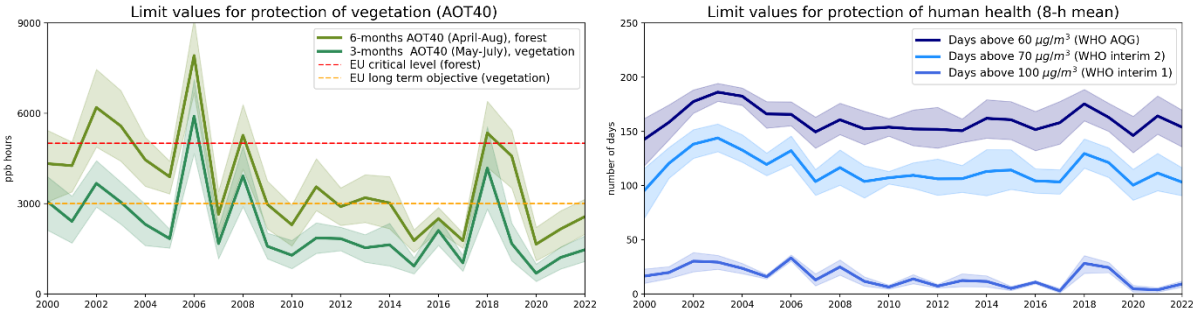

Figure 4.3:. Average trends in different ozone matrixes relevant for protection of vegetation (left, 7 sites) and health (right, 6 sites) at Norwegian background sites 2000-2022. The solid line in the trend plots indicate the average annual mean concentrations for all the sites and the shaded area the 90% confidence interval of the means.

4.4 Summary of trends

A summary of the average relative trends covered in this report is illustrated in the box plot in Figure 4.4. The average trends for the different sites and compounds are found in Appendix B. It is clear reduction for most of the components the last 20 years. The reductions are also seen for the shorter latter period from 2010(11), but there are larger variations between the sites, thus larger spread in the box plots, which is also reflected in less significant trend for this period. I.e., for the ozone metrics there are no significant trends for 2010-2022 (Table B.2).

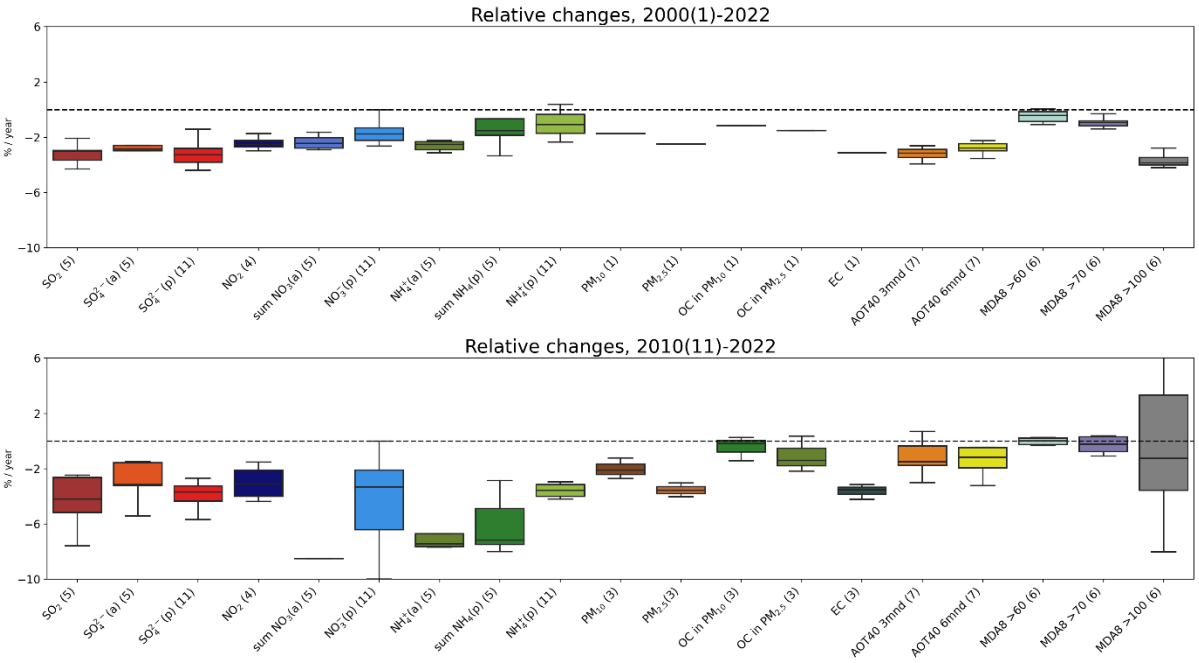

Figure 4.4: Average relative trends (Sen-Theil slope estimates) in annual levels for the period 2000(1)-2022 (top) and 2010(11)-2022 (bottom). Number of sites in the parentheses. The box plots represent the 50th, 25th, and 75th percentiles and the whiskers lie within the 1.5 inter-quartile ranges for the trends of all the sites, including those with not significant trends.

5 References

Aas, W., Berglen, T. F., Eckhardt, S., Fiebig, M., Solberg, S., Yttri, K.E. (2022) Monitoring of long-range transported air pollutants in Norway. Annual Report 2021. (NILU rapport 18/2022). Kjeller: NILU

Colette, A., Solberg, S., Aas, W., Walker, S.E. (2021) Understanding Air Quality Trends in Europe. Focus on the relative contribution of changes in emission of activity sectors, natural fraction and meteorological variability. Kjeller, ETC/ATNI (EIONET Report – ETC/ATNI 2020/8). https://www.eionet.europa.eu/etcs/etc-atni/products/etc-atni-reports/etc-atni-report-08-2020-understanding-air-quality-trends-in-europe-focus-on-the-relative-contribution-of-changes-in-emission-of-activity-sectors-natural-fraction-and-meteorological-variability

Berglen, T.F., Nilsen, A.-C., Vadset, M., Uggerud, H.T., Bjørklund, M., Andresen, E. (2022) Grenseområdene Norge-Russland. Luft- og nedbørkvalitet, årsrapport 2021. Kjeller: NILU (Miljødirektoratet rapport, M-2321/2022) (NILU rapport 22/2022).

EMEP (2021) Transboundary particulate matter, photo-oxidants, acidification and eutrophication components. Joint MSC-W & CCC & CEIP Report Oslo, Norwegian Meteorological Institute (EMEP Status Report 1/2021).

EMEP (2022) Transboundary particulate matter, photo-oxidants, acidification and eutrophication components. Joint MSC-W & CCC & CEIP Report Oslo, Norwegian Meteorological Institute (EMEP Status Report 1/2022).
https://emep.int/publ/reports/2022/EMEP_Status_Report_1_2022.pdf

EU (2008) Directive 2008/50/EC of the European Parliament and of the Council of 21 May 2008 on ambient air quality and cleaner air for Europe. *Off. J. Eur. Com.,* L 141, 11/06/2008, 1-44.

Eurostat (2023) Statistics from https://ec.europa.eu/eurostat, downloaded 5 July 2023

FHI (2013) Luftkvalitetskriterier. Virkninger av luftforurensning på helse. Oslo: Nasjonalt folkehelseinstitutt (Rapport, 2013:9).

FHI (2023) Nye luftkvalitetskriterier for svevestøv og nitrogendioksid, Folkehelseinstituttet. https://www.fhi.no/meldinger/nye-luftkvalitetskriterier-for-svevestov-og-nitrogendioksid/ (updated 09.06.2023)

Gilbert, R.O. (1987) Statistical methods for environmental pollution monitoring. New York: Van Nostrand Reinhold Co.

Hellen, H. (2023). Tenax TA tube results from EMEP intensive measurement period of 2022. Presentation at the EMEP TFMM, 10-12 May Warsaw, Poland.

Lewis R. B., Aas, W., Denby, B., Hjellbrekke A.G., Mu Q., Simpson, D., Ytre-Eide, M., Fagerli, H. (2023) Deposition of sulfur and nitrogen in Norway 2017-2021 (MET report 03/2023).

Mills, G., Pleijel, H., Braun, S., Büker, P., Bermejo, V., Calvo, E., Danielsson, H., Emberson, L., González Fernández, I., Grünhage L., Harmens, H., Hayes, F., Karlsson, P.-E., Simpson, D. (2011) New stomatal flux-based critical levels for ozone effects on vegetation. *Atmos. Environ., 45*, 5064-5068. https://doi.org/10.1016/j.atmosenv.2011.06.009

Pisso, I., Sollum, E., Grythe, H., Kristiansen, N. I., Cassiani, M., Eckhardt, S., Arnold, D., Morton, D., Thompson, R. L., Groot Zwaaftink, C. D., Evangeliou, N., Sodemann, H., Haimberger, L., Henne, S.,

Brunner, D., Burkhart, J. F., Fouilloux, A., Brioude, J., Philipp, A., Seibert, P., Stohl, A. (2019) The Lagrangian particle dispersion model FLEXPART version 10.4. *Geosci. Model Dev., 12*, 4955–4997. https://doi.org/10.5194/gmd-12-4955-2019.

Platt, S. M., Hov, Ø., Berg, T., Breivik, K., Eckhardt, S., Eleftheriadis, K., Evangeliou, N., Fiebig, M., Fisher, R., Hansen, G., Hansson, H.-C., Heintzenberg, J., Hermansen, O., Heslin-Rees, D., Holmén, K., Hudson, S., Kallenborn, R., Krejci, R., Krognes, T., Larssen, S., Lowry, D., Lund Myhre, C., Lunder, C., Nisbet, E., Nizzetto, P. B., Park, K.-T., Pedersen, C. A., Aspmo Pfaffhuber, K., Röckmann, T., Schmidbauer, N., Solberg, S., Stohl, A., Ström, J., Svendby, T., Tunved, P., Tørnkvist, K., van der Veen, C., Vratolis, S., Yoon, Y. J., Yttri, K. E., Zieger, P., Aas, W., Tørseth, K. (2022) Atmospheric composition in the European Arctic and 30 years of the Zeppelin Observatory, Ny-Ålesund. *Atmos. Chem. Phys., 22,* 3321–3369. https://doi.org/10.5194/acp-22-3321-2022

Saffari, A., Daher, N., Samara, C., Voutsa, D., Kouras, A., Manoli, E., Karagkiozidou, O., Vlachokostas, C., Moussiopoulos, N., Shafer, M. M., Schauer, J. J., Sioutas, C. (2013) Increased Biomass Burning Due to the Economic Crisis in Greece and Its Adverse Impact on Wintertime Air Quality in Thessaloniki. *Environ. Sci. Technol., 47,* 13313–13320. https://doi.org/10.1021/es403847h.

Timmermann, T., Børja, I., Clarke, N., Eriksen, R-, Gohli, J., Hylen, G., Jepsen, J. U., Krokene, P., Lange, H., Meissner, H., Nagy, N. E., Nordbakken, J.-F., Solberg, S. Solheim, H., Vindstad, O. P. L., Økland, B., Aas. W. (2023) The state of health of Norwegian forests. Results from the national forest damage monitoring 2021 (NIBIO rapport, 9/39/2023). In Norwegian.

Tørseth, K., Aas, W., Breivik, K., Fjæraa, A.M., Fiebig, M., Hjellbrekke, A.G., Myhre, C.L., Solberg, S., Yttri, K.E. (2012) Introduction to the European Monitoring and Evaluation Programme (EMEP) and observed atmospheric composition change during 1972–2009. *Atmos. Chem. Phys. 12*, 5447-5481. https://doi.org/10.5194/acp-12-5447-2012

UN/ECE (1999) The 1999 Gothenburg Protocol to the 1979 convention on long-range transboundary air pollution to abate acidification, eutrophication, and ground-level ozone. http://www.unece.org/env/lrtap/multi_h1.htm.

WHO (2021) WHO Global Air Quality Guidelines, updated September 2021. https://www.who.int/news-room/questions-and-answers/item/who-global-air-quality-guidelines

Yttri, K. E., Canonaco, F., Eckhardt, S., Evangeliou, N., Fiebig, M., Gundersen, H., Hjellbrekke, A.-G., Lund Myhre, C., Platt, S. M., Prévôt, A. S. H., Simpson, D., Solberg, S., Surratt, J., Tørseth, K., Uggerud, H., Vadset, M., Wan, X., Aas, W. (2021) Trends, composition, and sources of carbonaceous aerosol at the Birkenes Observatory, northern Europe, 2001–2018. *Atmos. Chem. Phys., 21,* 7149–7170 https://doi.org/10.5194/acp-21-7149-2021.

Yttri, K. E., Bäcklund, A., Conen, F., Eckhardt, S., Evangeliou, N., Fiebig, M., Kasper-Giebl, A., Gold, A., Gundersen, H., Myhre, C. L., Platt, S. M., Simpson, D., Surratt, J. D., Szidat, S., Rauber, M., Tørseth, K., Ytre-Eide, M. A., Zhang, Z., Aas, W. (2023) Composition and sources of carbonaceous aerosol in the European Arctic at Zeppelin Observatory, Svalbard. EGUsphere [preprint], https://doi.org/10.5194/egusphere-2023-615.

Appendix A

Annual and monthly mean concentrations

Table A.1. Annual volume weighted mean concentrations of inorganic ions in precipitation in 2022. (ssc= sea salt corrected, tot = total)

Site	pH	ssc SO_4 mg S/l	tot SO_4 mg S/l	NO_3 mg N/l	NH_4 mg N/l	Ca mg/l	K mg/l	Mg mg/l	Na mg/l	Cl mg/l	mm
Birkenes	5.042	0.104	0.213	0.24	0.225	0.14	0.076	0.144	1.302	2.229	1618
Vatnedalen	5.567	0.120	0.182	0.119	0.127	0.266	0.162	0.077	1.173	1.438	767
Treungen	5.070	0.074	0.102	0.174	0.092	0.121	0.043	0.042	0.344	0.588	1028
Løken	5.271	0.117	0.171	0.272	0.293	0.204	0.254	0.101	0.645	1.091	551
Hurdal	5.123	0.103	0.125	0.192	0.170	0.094	0.061	0.028	0.242	0.407	930
Osen (forest)	5.473	0.097	0.116	0.087	0.139	0.021	0.105	0.004	0.204	0.581	707
Brekkebygda	5.131	0.078	0.093	0.156	0.098	0.075	0.072	0.023	0.204	0.324	845
Vikedal	5.454	0.07	0.263	0.133	0.183	0.213	0.146	0.288	2.308	4.069	2756
Nausta	5.427	0.047	0.169	0.074	0.11	0.132	0.091	0.173	1.459	2.579	2502
Kårvatn	5.519	0.038	0.205	0.061	0.102	0.155	0.132	0.229	1.973	3.473	1552
Høylandet	5.774	0.042	0.223	0.046	0.307	0.31	0.143	0.285	2.158	3.782	960
Tustervatn	5.473	0.035	0.125	0.055	0.094	0.101	0.072	0.123	1.035	1.841	1305
Svanvik	5.003	0.158	0.213	0.082	0.063	0.117	0.057	0.085	0.653	1.178	398
Ny-Ålesund	5.430	0.074	0.429	0.065	0.121	0.503	0.184	0.564	4.246	7.448	340

Table A.2. Annual wet deposition of inorganic components in 2022. (ssc= sea salt corrected, tot = total).

Site	H^+	ssc SO_4 mg S/m^2	tot SO_4 mg S/m^2	NO_3 mg N/m^2	NH_4 mg N/m^2	Ca mg /m^2	K mg /m^2	Mg mg /m^2	Na mg /m^2	Cl mg /m^2	mm
Birkenes	14683	169	344	389	364	227	122	233	2107	3607	1618
Vatnedalen	2078	92	140	91	97	204	124	59	899	1102	767
Treungen	8752	76	105	179	95	125	44	43	354	604	1028
Løken	2951	64	94	150	161	112	140	56	355	601	551
Hurdal	7010	96	116	178	158	88	57	26	225	379	930
Osen (forest)	2375	69	82	62	98	15	74	3	144	411	707
Brekkebygda	6254	66	79	132	83	64	61	19	172	273	845
Vikedal	9692	192	725	365	505	588	403	793	6362	11215	2756
Nausta	9368	118	423	186	275	330	228	432	3652	6453	2502
Kårvatn	4700	59	318	95	158	240	204	355	3063	5391	1552
Høylandet	1615	40	214	44	295	298	138	274	2071	3630	960
Tustervatn	4385	46	163	71	122	131	94	160	1350	2401	1305
Svanvik	3953	63	85	33	25	47	23	34	260	469	398
Ny-Ålesund	1264	25	146	22	41	171	63	192	1444	2534	340

Table A.3. Annual mean concentrations of inorganic components in air in 2022.

Site	SO_2	SO_4^{2-}	NO_2	sum of (HNO_3 +NO_3^-)	NO_3^-	sum of (NH_3 + NH_4^+)	NH_4^+	Mg^{2+}	Ca^{2+}	K^+	Cl^-	Na^+
	µg-S/m³	µg-S/m³	µg-N/m³	µg-N/m³	µg-N/m³	µg-N/m³	µg-N/m³	µg/m³	µg/m³	µg/m³	µg/m³	µg/m³
Birkenes II	0.056	0.175	0.245	0.153	0.129	0.311	0.14	0.06	0.048	0.043	0.682	0.522
Hurdal	0.022	0.102	0.319	0.082	0.067	0.251	0.072	0.017	0.030	0.026	0.147	0.152
Kårvatn	0.022	0.087	0.133	0.035	0.023	0.550	0.029	0.027	0.035	0.025	0.303	0.215
Tustervatn	0.021	0.081	0.076	0.03	0.019	0.410	0.035	0.025	0.019	0.015	0.349	0.231
Zeppelin	0.083	0.130	-	0.025	0.015	0.235	0.037	0.033	0.025	0.036	0.371	0.256

Table A.4. Annual mean concentrations of aerosol mass and carbonaceous aerosols in 2022.

	PM_{10}					$PM_{2.5}$			
	PM_{10} mass	OC	EC	TC	Levoglucosan	$PM_{2.5}$ mass	OC	EC	TC
	µg/m³	µg-C/m³	µg-C/m³	µg-C/m³	ng/m³	µg/m³	µg-C/m³	µg-C/m³	µg-C/m³
Birkenes II	4.3	0.75	0.06	0.81	8.8	2.2	0.55	0.08	0.61
Hurdal	4.2	1.12	0.09	1.22		2.4	0.67	0.08	0.75
Kårvatn	2.6	0.64	0.04	0.68		1.2	0.42	0.04	0.45
Zeppelin		0.150	0.015	0.165					

Table A.5. Monthly and annual volume weighted mean pH in precipitation in 2022.

SITE	JAN	FEB	MAR	APR	MAY	JUN	JUL	AUG	SEP	OCT	NOV	DEC	2022
Birkenes	4.81	5.26	6.30	5.26	5.27	5.20	5.14	5.28	5.12	5.08	4.92	5.06	5.04
Vatnedalen	5.36	5.51	5.81	5.87	5.46	5.67	5.54	5.75	5.74	5.72	5.89	5.39	5.57
Treungen	4.76	5.21	6.59	5.72	5.08	5.36	5.14	5.18	5.09	5.06	4.98	5.03	5.07
Løken	5.27	5.39	5.63	6.49	5.35	5.43	5.38	5.82	5.21	5.50	5.22	4.99	5.27
Hurdal	4.77	5.27	5.23	6.08	5.41	5.24	5.32	5.31	5.09	4.95	4.98	5.10	5.12
Osen (forest)	5.44	5.55	5.72	5.40	5.35	5.34	5.58	5.71	5.34	5.37	5.50	5.57	5.47
Brekkebygda	5.12	5.19	5.75	6.18	5.31	5.10	5.30	5.22	5.39	5.00	5.03	4.99	5.13
Vikedal	5.45	5.47	5.95	5.77	5.49	5.24	5.42	5.49	5.53	5.54	5.33	5.54	5.45
Nausta	5.53	5.38	5.61	5.63	5.50	5.42	5.43	5.36	5.49	5.36	5.33	5.36	5.43
Kårvatn	5.56	5.49	5.65	5.78	5.33	5.73	5.40	5.46	5.58	5.62	5.55	5.52	5.52
Høylandet	6.07	5.95	6.36	5.93	5.60	5.96	5.64	5.33	5.56	5.80	6.00	6.10	5.77
Tustervatn	5.60	5.55	5.67	5.61	5.49	5.39	5.30	5.30	5.44	5.52	5.49	5.35	5.47
Svanvik	5.19	5.00	4.85	4.80	5.08	5.09	4.74	5.16	5.18	5.27	4.95	4.88	5.00
Ny-Ålesund	5.84	5.03	5.55	5.72	5.31	5.79	6.15	5.43	5.34	5.80	5.48	5.31	5.43

Table A.6. Monthly and annual volume weighted average concentrations of sulfate (sea salt corrected) in precipitation in 2022. Unit: mg S/L.

SITE	JAN	FEB	MAR	APR	MAY	JUN	JUL	AUG	SEP	OCT	NOV	DEC	2022
Birkenes	0.081	0.030	0.644	0.057	0.202	0.146	0.168	0.117	0.092	0.079	0.109	0.055	0.104
Vatnedalen	0.020	0.040	0.210	0.420	0.169	0.324	0.344	0.327	0.137	0.145	0.040	0.079	0.120
Treungen	0.141	0.021	0.355	0.471	0.164	0.081	0.155	0.099	0.061	0.065	0.067	0.025	0.074
Løken	0.074	0.034	0.428	0.516	0.216	0.257	0.171	0.406	0.108	0.073	0.087	0.041	0.117
Hurdal	0.107	0.017	0.790	0.226	0.138	0.175	0.090	0.117	0.070	0.068	0.098	0.038	0.103
Osen (forest)	0.040	0.016	0.010	0.120	0.125	0.172	0.112	0.120	0.062	0.070	0.061	0.030	0.097
Brekkebygda	0.049	0.015	0.810	0.487	0.167	0.116	0.079	0.126	0.031	0.056	0.087	0.041	0.078
Vikedal	0.011	0.020	0.255	0.123	0.137	0.173	0.126	0.133	0.051	0.061	0.028	0.025	0.070
Nausta	0.006	-0.002	0.107	0.087	0.075	0.147	0.086	0.092	0.019	0.039	0.011	0.005	0.047
Kårvatn	-0.01	0.006	0.024	0.092	0.100	0.165	0.084	0.051	0.007	0.025	0.003	0.020	0.038
Høylandet	0.007	0.006	0.025	0.058	0.016	0.177	0.094	0.076	0.003	0.008	0.009	0.025	0.042
Tustervatn	0.004	0.008	0.053	0.042	0.069	0.093	0.068	0.068	0.015	0.013	0.005	0.006	0.035
Svanvik	0.037	0.114	0.274	0.612	0.306	0.242	0.299	0.068	0.107	0.041	0.129	0.061	0.158
Ny-Ålesund	0.048	0.330	0.056	0.171	0.233	0.402	0.452	0.016	-0.005	0.086	0.028	0.011	0.074

Table A.7. Monthly and annual volume weighted average concentrations of nitrate in precipitation in 2022. Unit: mg N/L.

SITE	JAN	FEB	MAR	APR	MAY	JUN	JUL	AUG	SEP	OCT	NOV	DEC	2022
Birkenes	0.314	0.153	1.172	0.161	0.293	0.217	0.312	0.166	0.190	0.239	0.261	0.184	0.240
Vatnedalen	0.084	0.085	0.527	0.467	0.193	0.190	0.116	0.212	0.148	0.104	0.121	0.081	0.119
Treungen	0.454	0.134	0.691	0.954	0.213	0.158	0.213	0.128	0.163	0.182	0.163	0.125	0.174
Løken	0.273	0.192	1.250	1.280	0.316	0.296	0.265	0.654	0.348	0.251	0.255	0.219	0.272
Hurdal	0.340	0.145	1.365	0.515	0.173	0.224	0.135	0.127	0.125	0.217	0.240	0.159	0.192
Osen (forest)	0.116	0.104	0.100	0.160	0.163	0.186	0.076	0.072	0.029	0.056	0.089	0.120	0.087
Brekkebygda	0.193	0.128	1.873	1.282	0.230	0.115	0.084	0.103	0.011	0.120	0.209	0.199	0.156
Vikedal	0.131	0.104	0.721	0.205	0.169	0.200	0.122	0.133	0.095	0.087	0.117	0.108	0.133
Nausta	0.048	0.072	0.280	0.110	0.073	0.083	0.132	0.091	0.005	0.061	0.040	0.034	0.074
Kårvatn	0.082	0.022	0.040	0.069	0.100	0.105	0.054	0.046	0.009	0.011	0.005	0.050	0.061
Høylandet	0.043	0.046	0.084	0.087	0.027	0.073	0.020	0.015	-	0.049	0.063	0.047	0.046
Tustervatn	0.045	0.042	0.066	0.069	0.089	0.067	0.070	0.048	0.033	0.035	0.030	0.047	0.055
Svanvik	0.098	0.098	0.111	0.470	0.132	0.092	0.008	0.025	0.024	0.091	0.194	0.198	0.082
Ny-Ålesund	0.059	0.046	0.066	0.047	0.094	0.219	0.295	0.025	0.044	0.052	0.081	0.041	0.065

Table A.8. Monthly and annual volume weighted average concentrations of ammonium in precipitation in 2022. Unit: mg N/L.

SITE	JAN	FEB	MAR	APR	MAY	JUN	JUL	AUG	SEP	OCT	NOV	DEC	2022
Birkenes	0.170	0.116	2.024	0.089	0.423	0.199	0.225	0.207	0.146	0.201	0.243	0.130	0.225
Vatnedalen	0.052	0.055	0.618	1.685	0.225	0.243	0.101	0.661	0.035	0.077	0.081	0.066	0.127
Treungen	0.275	0.039	1.098	0.728	0.187	0.083	0.149	0.120	0.064	0.065	0.092	0.027	0.092
Løken	0.259	0.159	1.466	1.586	0.193	0.466	0.319	1.278	0.381	0.183	0.345	0.119	0.293
Hurdal	0.197	0.064	2.239	0.852	0.317	0.306	0.121	0.180	0.072	0.105	0.132	0.067	0.170
Osen (forest)	0.057	0.046	0.072	0.228	0.235	0.266	0.145	0.161	0.071	0.078	0.111	0.080	0.139
Brekkebygda	0.089	0.025	2.459	2.204	0.269	0.085	0.037	0.178	0.016	0.032	0.113	0.077	0.098
Vikedal	0.140	0.159	1.092	0.521	0.266	0.261	0.145	0.213	0.078	0.142	0.119	0.172	0.183
Nausta	0.055	0.080	0.441	0.228	0.135	0.238	0.155	0.113	0.012	0.085	0.015	0.063	0.110
Kårvatn	0.102	0.056	0.046	0.294	0.112	0.662	0.073	0.035	0.011	0.022	0.009	0.077	0.102
Høylandet	0.417	0.418	0.584	0.358	0.121	0.236	0.042	0.039	0.066	0.275	0.356	0.728	0.307
Tustervatn	0.062	0.055	0.167	0.127	0.173	0.184	0.098	0.078	0.044	0.051	0.054	0.050	0.094
Svanvik	0.041	0.071	0.094	0.342	0.134	0.324	0.054	0.010	0.018	0.013	0.059	0.038	0.063
Ny-Ålesund	0.166	0.126	0.135	0.048	0.084	0.131	0.266	0.067	0.243	0.284	0.096	0.060	0.121

Table A.9. Monthly and annual precipitation amount at Norwegian background stations in 2022. Unit: mm.

SITE	JAN	FEB	MAR	APR	MAY	JUN	JUL	AUG	SEP	OCT	NOV	DEC	2022
Birkenes	64	139	18	8	76	60	59	110	164	184	566	171	1618
Vatnedalen	102	137	6	5	36	25	36	42	60	162	77	78	767
Treungen	19	73	5	7	31	57	48	82	203	149	248	105	1028
Løken	24	75	2	3	25	60	72	13	38	75	76	89	551
Hurdal	23	72	4	10	68	121	82	102	106	120	144	78	930
Osen (forest)	18	14	6	21	47	59	129	147	84	114	58	10	707
Brekkebygda	16	55	2	3	48	78	40	74	148	123	196	62	845
Vikedal	390	402	36	47	211	211	234	196	179	365	228	257	2756
Nausta	526	313	88	44	165	199	236	279	97	252	151	154	2502
Kårvatn	355	19	21	17	131	101	204	119	306	119	49	112	1552
Høylandet	152	137	102	26	23	60	126	107	14	142	28	43	960
Tustervatn	213	103	179	36	96	69	111	137	40	160	74	86	1305
Svanvik	26	17	17	6	33	22	71	72	52	50	7	25	398
Ny-Ålesund	10	9	60	9	32	9	4	39	35	16	62	55	340

Table A.10 Monthly and annual mean concentrations of sulfur dioxide in air in 2022. Unit: µg S/m3.

SITE	JAN	FEB	MAR	APR	MAY	JUN	JUL	AUG	SEP	OCT	NOV	DEC	2022
Birkenes II	0.032	0.041	0.104	0.057	0.077	0.100	0.099	0.064	0.018	0.025	0.025	0.03	0.056
Hurdal	0.014	0.011	0.054	0.02	0.025	0.041	0.028	0.021	0.01	0.011	0.012	0.013	0.022
Kårvatn	0.015	0.063	0.164	0.019	0.028	0.019	0.03	0.016	0.015	0.01	0.014	0.019	0.022
Tustervatn	0.015	0.021	0.022	0.023	0.021	0.034	0.018	0.033	0.012	0.011	0.019	0.027	0.021
Zeppelin	0.054	0.109	0.176	0.167	0.06	0.033	0.041	0.013	0.026	0.028	0.013	0.262	0.083

Table A.11. Monthly and annual mean concentrations of sulfate in aerosol in 2022. Unit: µg S/m3.

SITE	JAN	FEB	MAR	APR	MAY	JUN	JUL	AUG	SEP	OCT	NOV	DEC	2022
Birkenes II	0.102	0.113	0.272	0.111	0.183	0.289	0.231	0.259	0.124	0.154	0.154	0.099	0.175
Hurdal	0.065	0.046	0.185	0.064	0.112	0.162	0.126	0.163	0.082	0.067	0.075	0.067	0.102
Kårvatn	0.043	0.298	0.116	0.090	0.100	0.139	0.132	0.098	0.060	0.025	0.037	0.046	0.087
Tustervatn	0.055	0.059	0.087	0.083	0.092	0.145	0.076	0.137	0.072	0.043	0.046	0.075	0.081
Zeppelin	0.151	0.174	0.191	0.229	0.215	0.202	0.139	0.048	0.039	0.033	0.026	0.112	0.130

Table A.12. Monthly and annual mean concentrations of nitrogen dioxide in 2022. Unit: µg N/m3.

SITE	JAN	FEB	MAR	APR	MAY	JUN	JUL	AUG	SEP	OCT	NOV	DEC	2022
Birkenes II	0.259	0.293	0.339	0.136	0.194	0.170	0.171	0.207	0.163	0.352	0.454	0.202	0.245
Hurdal	0.749	0.503	0.489	0.160	0.300	0.203	0.150	0.201	0.203	0.330	0.254	0.291	0.319
Kårvatn	0.165	0.110	-	0.090	0.072	0.092	0.120	0.144	0.071	0.137	0.169	0.223	0.133
Tustervatn	0.093	0.108	0.086	0.087	0.075	0.089	0.039	0.057	0.080	0.101	0.054	0.043	0.076

Table A.13. Monthly and annual mean concentrations of sum of nitrate and nitric acid in air in 2022. Unit: µg N/m3.

SITE	JAN	FEB	MAR	APR	MAY	JUN	JUL	AUG	SEP	OCT	NOV	DEC	2022
Birkenes II	0.080	0.099	0.514	0.102	0.132	0.186	0.156	0.148	0.078	0.141	0.133	0.061	0.153
Hurdal	0.095	0.076	0.233	0.032	0.077	0.067	0.080	0.081	0.048	0.060	0.046	0.087	0.082
Kårvatn	0.020	0.168	0.096	0.030	0.038	0.029	0.042	0.029	0.021	0.022	0.022	0.022	0.035
Tustervatn	0.023	0.026	0.074	0.039	0.035	0.025	0.020	0.026	0.021	0.023	0.021	0.024	0.030
Zeppelin	0.027	0.024	0.026	0.030	0.036	0.021	0.024	0.020	0.020	0.020	0.020	0.032	0.025

Table A.14. Monthly and annual mean concentrations of sum of ammonium and ammonia in air in 2022. Unit: µg N/m3.

SITE	JAN	FEB	MAR	APR	MAY	JUN	JUL	AUG	SEP	OCT	NOV	DEC	2022
Birkenes II	0.089	0.201	0.856	0.382	0.345	0.43	0.35	0.386	0.153	0.209	0.211	0.109	0.311
Hurdal	0.225	0.131	0.45	0.173	0.283	0.342	0.268	0.305	0.247	0.234	0.153	0.185	0.251
Kårvatn	0.297	0.597	0.602	0.685	0.575	0.728	0.899	0.777	0.377	0.194	0.221	0.728	0.55
Tustervatn	0.258	0.171	0.412	0.393	0.593	0.781	0.442	0.509	0.383	0.573	0.211	0.162	0.41
Zeppelin	0.146	0.233	0.293	0.165	0.238	0.256	0.623	0.196	0.173	0.201	0.105	0.16	0.235

Table A.15. Monthly and annual mean of aerosol mass concentrations in 2022. Unit: µg/m3.

SITE	JAN	FEB	MAR	APR	MAY	JUN	JUL	AUG	SEP	OCT	NOV	DEC	2022
	PM_{10}												
Birkenes II (1h)	3.240	4.741	7.513	3.891	4.541	5.730	5.094	5.739	3.608	5.402	4.319	2.468	4.698
Birkenes II (1w)	3.321	4.480	9.769	2.988	3.862	6.185	3.820	4.768	4.062	4.453	1.890	1.751	4.294
Hurdal	3.311	3.242	7.499	2.825	4.476	5.539	4.172	5.296	3.975	4.062	2.418	2.852	4.152
Kårvatn	1.909	1.030	1.131	2.094	3.358	4.896	3.058	2.976	4.014	1.720	1.571	1.044	2.604
	$PM_{2.5}$												
Birkenes II	1.713	1.681	6.376	1.821	2.078	2.502	2.413	2.775	1.607	1.295	0.554	1.128	2.230
Hurdal	2.513	1.661	4.743	1.487	2.210	3.107	2.396	2.728	1.797	1.575	1.345	2.494	2.364
Kårvatn	0.532	0.523	0.719	1.355	1.164	2.509	1.624	1.897	1.431	0.797	0.786	0.765	1.245

Table A.16. Monthly and annual mean concentrations of organic carbon (OC) in 2022. Unit: µgC/m3.

SITE	JAN	FEB	MAR	APR	MAY	JUN	JUL	AUG	SEP	OCT	NOV	DEC	2022
	OC in PM_{10}												
Birkenes II	0.408	0.258	1.286	0.648	0.657	0.961	0.945	1.137	0.986	0.801	0.399	0.383	0.749
Hurdal	0.949	0.452	1.309	0.576	1.163	1.829	1.350	1.671	1.492	1.381	0.622	0.625	1.124
Kårvatn	0.196	0.189	0.125	0.378	0.550	1.117	0.998	1.050	0.812	0.692	0.434	0.290	0.641
Zeppelin	0.311	0.223	0.191	0.157	0.268	0.159	0.150	0.074	0.070	0.084	0.029	0.105	0.150
	OC in $PM_{2.5}$												
Birkenes II	0.340	0.239	1.197	0.555	0.525	0.734	0.711	0.763	0.475	0.356	0.254	0.360	0.553
Hurdal	0.727	0.415	1.113	0.427	0.669	0.942	0.792	0.832	0.601	0.418	0.375	0.652	0.666
Kårvatn	0.146	0.171	0.192	0.379	0.449	0.834	0.566	0.535	0.495	0.339	0.282	0.244	0.416

Table A.17. Monthly and annual mean concentrations of elemental carbon (EC) in 2022. Unit: µgC/m3.

SITE	JAN	FEB	MAR	APR	MAY	JUN	JUL	AUG	SEP	OCT	NOV	DEC	2022
	EC in PM_{10}												
Birkenes II	0.050	0.026	0.192	0.057	0.030	0.050	0.049	0.056	0.054	0.050	0.077	0.059	0.063
Hurdal	0.185	0.074	0.193	0.061	0.057	0.050	0.049	0.069	0.087	0.086	0.064	0.117	0.091
Kårvatn	0.020	0.025	0.011	0.023	0.018	0.027	0.026	0.038	0.050	0.055	0.053	0.054	0.036
Zeppelin	0.034	0.035	0.033	0.024	0.017	0.007	0.006	0.003	0.002	0.003	0.001	0.017	0.015
	EC in $PM_{2.5}$												
Birkenes II	0.048	0.028	0.163	0.049	0.032	0.046	0.046	0.051	0.042	0.039	0.064	0.057	0.056
Hurdal	0.152	0.074	0.170	0.050	0.050	0.044	0.047	0.057	0.064	0.072	0.060	0.136	0.082
Kårvatn	0.021	0.025	0.016	0.028	0.018	0.028	0.030	0.035	0.051	0.050	0.047	0.051	0.036

Table A.18. Monthly and annual mean concentrations of levoglucosan in PM_{10} in 2022. Unit: ng /m^3.

SITE	JAN	FEB	MAR	APR	MAY	JUN	JUL	AUG	SEP	OCT	NOV	DEC	2022
Birkenes II	19.97	9.16	28.15	10.13	2.64	2.32	1.63	1.48	4.09	6.53	1.23	17.79	8.80

Table A.19. Different matrices for ozone in 2022: The annual number of days with Daily Maximum 8-hour Average (MDA 8-h) exceeding different health indicators and thresholds, and Accumulated exposure over the threshold of 40 ppb (AOT40) during the growing season for forest (6 months: 1 April – 30 Sept.), semi-natural vegetation (1 May – 31 July) and the maximum hourly concentrations.

	MDA 8-h (nr of days)				AOT 40 (ppb hours)		Max hourly conc.	
Site	>60 μg/m^3	>70 μg/m^3	>100 μg/m^3	>120 μg/m^3	6 months, forest	3 months, vegetation	μg/m^3	Date
Birkenes II	177	128	16	3	4344	2846	157.2	20/07/2022
Hurdal	143	98	11	1	2251	1364	144.7	20/07/2022
Kårvatn	105	76	5	0	2416	1035	127.6	27/03/2022
Prestebakke	164	116	11	2	2907	1735	152.0	21/07/2022
Haukenes	151	105	7	1	3555	2104	145.2	20/07/2022
Sandve	196	131	12	2	2897	1707	177.4	19/07/2022
Tustervatn	145	93	8	0	2236	1074	112.1	06/05/2022
Svanvik[1]	84	58	0	0	957	258	109.0	18/03/2022
Zeppelin	147	80	1	0	935	516	103.2	27/05/2022

[1)]measurement started 14. February 2022

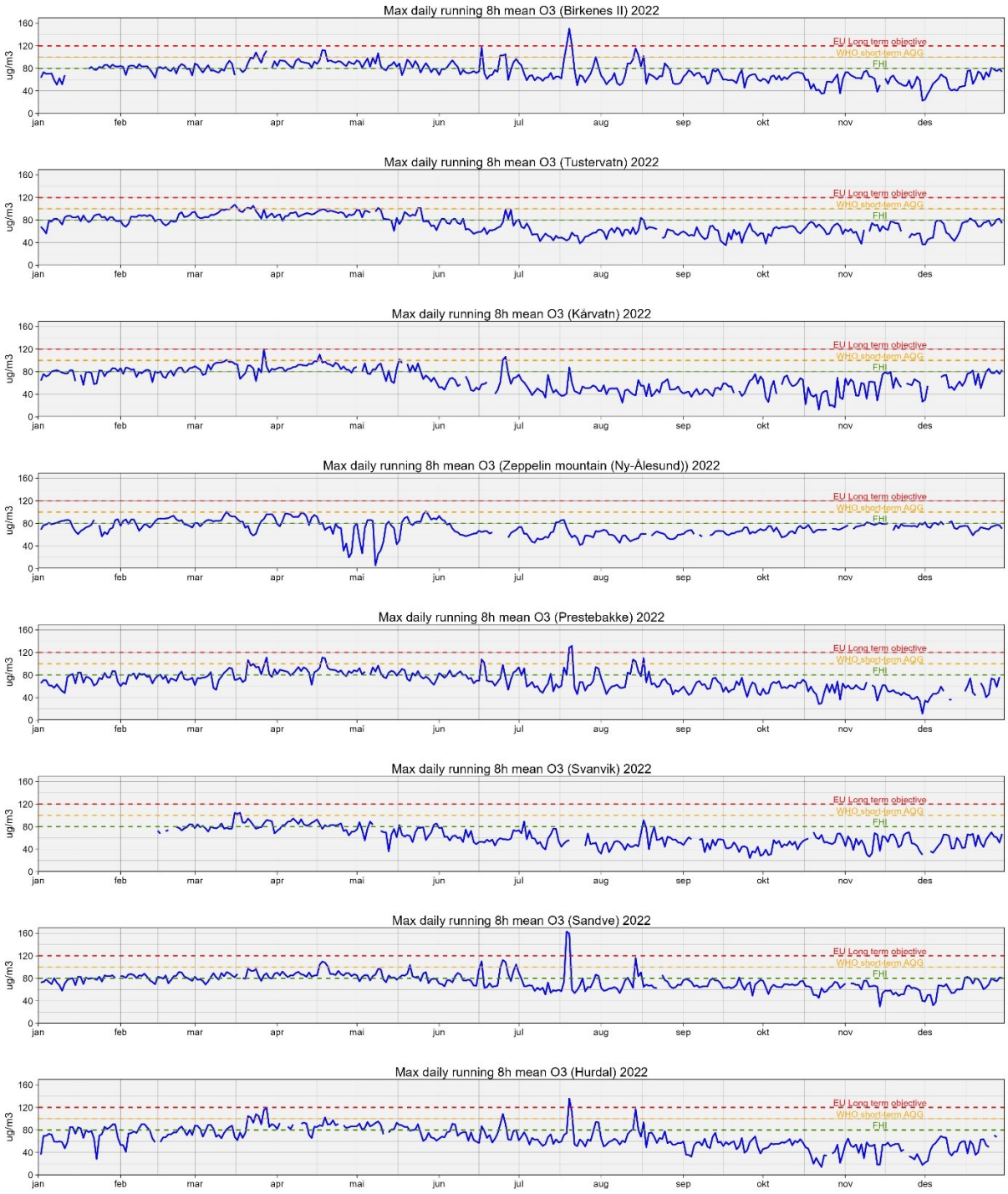

Figure A.1: Max daily running 8 h (MDA8) at Norwegian ozone sites in 2022 compared to threshold and target values set by EU (2008), WHO (2021) and FHI (2013)

Appendix B

Trend results

Table B.1. Absolute and relative change and corresponding 95% confidence intervals in annual concentrations for sulfur and nitrogen compounds in air and precipitation for 2000-2022 and 2010-2022. The number of sites with a significant outcome is provided.

		Nr of sites		Abs. change (mg/L or ug S(N)/m^3)/y		Relative change (%/y)	
component	period	tot	sign	slope	Conf. Interval.	slope	Conf. Interval.
SO_2	2000-2022	5	5	-0.003	(-0.005, -0.001)	-3.2	(-4.23, -2.17)
SO_2	2010-2022	5	3	-0.003	(-0.005, -0.001)	-4.41	(-7.01, -1.81)
SO_4^{2-} in aerosols	2000-2022	5	5	-0.008	(-0.014, -0.002)	-2.69	(-3.81, -1.57)
SO_4^{2-} in aerosols	2010-2022	5	3	-0.006	(-0.012, -0.0)	-2.97	(-4.96, -0.98)
SO_4^{2-} in precip.	2000-2022	11	11	-0.007	(-0.01, -0.004)	-3.28	(-3.75, -2.81)
SO_4^{2-} in precip.	2010-2022	10	5	-0.005	(-0.008, -0.002)	-3.49	(-4.47, -2.51)
NO_2	2000-2022	4	4	-0.012	(-0.029, 0.005)	-2.44	(-3.27, -1.61)
NO_2	2010-2022	4	3	-0.013	(-0.037, 0.011)	-3.02	(-5.13, -0.91)
NO_3^- in aerosol	2000-2022	5	0	-0.002	(-0.003, -0.001)	-2.4	(-4.01, -0.79)
NO_3^- in aerosol	2010-2022	5	5	-0.011	(-0.015, -0.007)	-8.13	(-10.46, -5.8)
sum(HNO_3 NO_3^-)	2000-2022	5	3	-0.004	(-0.007, -0.001)	-2.36	(-3.01, -1.71)
sum(HNO_3+NO_3^-)	2010-2022	5	5	-0.016	(-0.024, -0.008)	-8.35	(-10.12, -6.58)
NO_3^- in precip.	2000-2022	11	8	-0.004	(-0.006, -0.002)	-1.5	(-2.06, -0.94)
NO_3^- in precip.	2010-2022	10	5	-0.005	(-0.008, -0.002)	-2.35	(-3.38, -1.32)
NH_4^+ in aerosol	2000-2022	5	4	-0.005	(-0.009, -0.001)	-2.63	(-3.12, -2.14)
NH_4^+ in aerosol	2010-2022	5	4	-0.011	(-0.017, -0.005)	-6.74	(-8.56, -4.92)
sum(NH_4^++NH_3)	2000-2040	5	1	-0.011	(-0.029, 0.007)	-1.21	(-3.35, 0.93)
sum(NH_4^++NH_3)	2010-2022	5	3	-0.032	(-0.049, -0.015)	-6.08	(-8.77, -3.39)
NH_4^+ in precip	2000-2022	11	4	-0.003	(-0.005, -0.001)	-0.84	(-1.64, -0.04)
NH_4^+ in precip	2010-2022	10	7	-0.008	(-0.011, -0.005)	-3.22	(-4.18, -2.26)

Table B.2. Absolute and relative change and corresponding 95% confidence intervals in annual concentrations for different ozone matrixes for 2000-2022 and 2010-2022. The number of sites with a significant outcome is provided.

		Nr of sites		Abs. change (μg/m^3/y or ppb h/y)		Relative change (%/y)	
component	period	tot	sign	slope	Conf. Interval.	slope	Conf. Interval.
AOT_3mon	2000-2022	7	4	-80	(-122, -38)	-2.94	(-3.88, -2.0)
AOT_3mon	2010-2022	7	0	-20	(-43, 3)	-1.14	(-2.4, 0.12)
AOT_6mon	2000-2022	7	5	-129	(-179, -79)	-2.66	(-3.3, -2.02)
AOT_6mon	2010-2022	7	0	-35	(-93, 23)	-1.06	(-2.58, 0.46)
MDA8_6mon_100ug	2000-2022	6	4	-0.842	(-1.244, -0.44)	-3.68	(-4.23, -3.13)
MDA8_6mon_100ug	2010-2022	6	0	0.003	(-0.381, 0.387)	-0.66	(-6.21, 4.89)
MDA8_6mon_60ug	2000-2022	6	2	-0.827	(-1.595, -0.059)	-0.49	(-0.96, -0.02)
MDA8_6mon_60ug	2010-2022	6	0	0.05	(-0.995, 1.095)	-0.01	(-0.68, 0.66)
MDA8_6mon_70ug	2000-2022	6	2	-1.203	(-1.757, -0.649)	-0.93	(-1.34, -0.52)
MDA8_6mon_70ug	2010-2022	6	0	-0.228	(-0.944, 0.488)	-0.27	(-0.94, 0.4)

Table B.3. Average absolute and relative changes and corresponding 95% confidence intervals in annual concentrations for aerosol mass concentration, organic- and elemental carbon, and levoglucosan for 2000(1)-2022 and 2011-2022. Individual trends for the different sites and components are also provided.

				Absolute change		Relative change	
Site	Period	component	p_value	μg/m^3/y	Conf. Int.	%/y	Conf. Int.
Birkenes	2000-2022	PM_{10} mass conc.	0.0004	-0.116	(-0.163, -0.069)	-1.73	(-2.42, -1.03)
Birkenes	2000-2022	$PM_{2.5}$ mass conc.	0.00003	-0.107	(-0.139, -0.076)	-2.49	(-3.23, -1.76)
Birkenes	2000-2022	PM_{10}-$PM_{2.5}$ mass conc.	0.29	-0.019	(-0.06, 0.022)	-0.78	(-2.46, 0.93)
Birkenes	2001-2022	TC in PM_{10}	0.0057	-0.016	(-0.024, -0.007)	-1.43	(-2.16, -0.63)
Birkenes	2001-2022	TC in $PM_{2.5}$	0.0019	-0.015	(-0.023, -0.008)	-1.76	(-2.73, -0.88)
Birkenes	2001-2022	OC in PM_{10}	0.013	-0.011	(-0.02, -0.003)	-1.15	(-2.04, -0.35)
Birkenes	2001-2022	OC in $PM_{2.5}$	0.0080	-0.011	(-0.018, -0.003)	-1.53	(-2.48, -0.46)
Birkenes	2001-2022	OC in PM_{10}-$PM_{2.5}$	0.79	0	(-0.004, 0.003)	0	(-1.69, 1.29)
Birkenes	2001-2022	EC in PM_{10}	0.00003	-0.004	(-0.005, -0.003)	-3.12	(-3.72, -2.01)
Birkenes	2001-2022	EC in $PM_{2.5}$	0.0032	-0.003	(-0.005, -0.002)	-3.23	(-5.6, -1.7)
Birkenes	2011-2022	PM_{10} mass conc.	0.087	-0.156	(-0.281, -0.031)	-2.71	(-4.88, -0.54)
Hurdal	2011-2022	PM_{10} mass conc.	0.19	-0.055	(-0.157, 0.046)	-1.23	(-3.53, 1.04)
Kårvatn	2011-2022	PM_{10} mass conc.	0.24	-0.072	(-0.166, 0.022)	-2.11	(-4.87, 0.64)
		Average PM_{10}		-0.094	(-0.228, 0.04)	-2.02	(-3.87, -0.17)
Birkenes	2011-2022	$PM_{2.5}$ mass conc.	0.0049	-0.141	(-0.209, -0.073)	-4.03	(-5.97, -2.09)
Hurdal	2011-2022	$PM_{2.5}$ mass conc.	0.023	-0.1	(-0.181, -0.02)	-3.03	(-5.48, -0.61)
Kårvatn	2011-2022	$PM_{2.5}$ mass conc.	0.062	-0.093	(-0.188, 0.002)	-3.57	(-7.22, 0.08)
		Average $PM_{2.5}$		-0.111	(-0.175, -0.047)	-3.54	(-4.78, -2.3)
Birkenes	2011-2022	OC in PM_{10}	0.73	0.002	(-0.017, 0.022)	0.27	(-2.31, 2.86)
Hurdal	2011-2022	OC in PM_{10}	0.94	-0.002	(-0.028, 0.023)	-0.18	(-2.42, 2.05)
Kårvatn	2011-2022	OC in PM_{10}	0.19	-0.011	(-0.027, 0.006)	-1.42	(-3.45, 0.71)
		Average OC in PM_{10}		-0.004	(-0.021, 0.013)	-0.44	(-2.61, 1.73)
Birkenes	2011-2022	OC in $PM_{2.5}$	0.94	0.002	(-0.01, 0.014)	0.36	(-1.79, 2.6)
Hurdal	2011-2022	OC in $PM_{2.5}$	0.24	-0.011	(-0.027, 0.004)	-1.4	(-3.43, 0.55)
Kårvatn	2011-2022	OC in $PM_{2.5}$	0.12	-0.013	(-0.027, 0.001)	-2.17	(-4.5, 0.1)
		Average OC in $PM_{2.5}$		-0.007	(-0.027, 0.013)	-1.07	(-4.29, 2.15)
Birkenes	2011-2022	EC in PM_{10}	0.033	-0.003	(-0.005, -0.001)	-3.16	(-5.33, -1.05)
Hurdal	2011-2022	EC in PM_{10}	0.0075	-0.006	(-0.008, -0.004)	-4.23	(-5.93, -2.59)
Kårvatn	2011-2022	EC in PM_{10}	0.0075	-0.002	(-0.003, -0.001)	-3.51	(-6.09, -2.02)
		Average EC in PM_{10}		-0.004	(-0.009, 0.001)	-3.63	(-4.99, -2.27)
Birkenes	2011-2022	Levoglucosan in PM_{10}	0.0641	-0.262	(-0.473, -0.051)	-2.45	(-4.41, -0.48)

Appendix C

Detailed information of the monitoring programme

Table C.1: Site locations and station keepers for the background sites in 2022.

Stasjon	Fylke	m.o.h.	Bredde N	Lengde E	Start dato	Stasjonsholder	Adresse
Birkenes	Aust-Agder	190	58° 23'	8° 15'	nov-71	Olav Lien	4760 Birkeland
Birkenes II		219					
Vatnedalen	Aust-Agder	800	59° 30'	7° 26'	nov-73	Lilly Vatnedalen	4694 Bykle
Treungen	Telemark	270	59° 01'	8° 32'	sep-74	Per Ø. Stokstad	4860 Treungen
Haukenes	Telemark	20	59° 12'	9° 31'	apr-79		
Prestebakke	Østfold (VIken)	160	59° 00'	11° 32'	nov-85	NILU	2027 Kjeller
Løken	Akershus (VIken)	135	59° 48'	11° 27'	mar-72	Anne Mørch	1960 Løken
Hurdal	Akerhus (VIken)	300	60° 22’	11° 04’	jan-97	Thomas Sørlien	2090 Hurdal
Osen (forest)*	Innlandet	560	61° 17’	11° 51’	May-1987	NIBIO	2060 Osen
Brekkebygda	Buskerud (Viken)	390	60° 18'	9° 44'	des-97	Anton Brekka	3534 Sokna
Vikedal II	Rogaland	60	59° 32'	5° 58'	jan-84	Harald Leifsen	4210 Vikedal
Sandve	Rogaland	40	59° 12'	5° 12'	jun-96	Jan M. Jensen	4272 Sandve
Nausta	Vestland	230	61° 34'	5° 53'	des.84	Sverre Ullaland	6043 Naustdal
Kårvatn	Møre og Romsdal	210	62° 47'	8° 53'	feb-78	Erik Kårvatn	6645 Todalen
Høylandet	Trøndelag	60	64° 39'	12° 19’	feb-87	Jakob Olav Almås	7977 Høylandet
Tustervatn	Nordland	439	65° 50'	13° 55'	des-71	Are Tustervatn	8647 Bleikvassli
Svanvik	Finnmark	30	69°27'	30°02’	aug-86	NIBIO	9900 Kirkenes
Ny-Ålesund	Svalbard	8	78° 55'	11° 55'	1974	NP forskningsst.	9173 Ny-Ålesund
Zeppelin	Svalbard	474	78° 54'	11° 53'	sep-89	NP forskningsst.	9173 Ny-Ålesund

* Osen (forest) is part of the national forest damage monitoring conducted by NIBIO

Table C.2:Measurement programme at Norwegian background stations in 2022, including the environmental contaminants reported in Halvorsen et al. (2023) and observations from Osen (forest) which is part of the forest damage monitoring programme done by NIBIO

	Air							Precipitation			
	Hourly		Daily		Weekly		2d per week	Daily	Weekly		monthly
Stasjon	Metr.	Ozone	main	NO_2	$PM_{2,5,}$ PM_{10} + EC/OC	HM.	POPs	main	main	HM	POPs
Birkenes Vatnedalen	X	X	X	X	X	X[b]	X[d]	X	X	X[b]	X[e]
Treungen Haukenes		X							X		
Prestebakke Løken Hurdal	X	X X	X	X	X			X	X	X[a]	
Osen (forest)									X		
Brekkebygda									X		
Vikedal Sandve		X							X		
Nausta									X		
Kårvatn		X	X	X	X			X		X[a]	
Høylandet									X		
Tustervatn		X	X	X				X			
Svanvik		X							X	X	
Zeppelin, Ny-Ålesund	X	X	X		EC/OC	X[c]	X[g]		X		
Total number	3	8+1	5	4	3+1	2	2	4	10	4	1

Metr. = meteorology
main.precip = amount (mm), pH, conductivity, SO_4, NO_3, Cl, NH_4, Ca, K, Mg, Na
main air = SO_2, SO_4, HNO_3 + NO_3 ; NH_4+ NH_3, Ca, K, Mg, Na, Cl
HM [a] = Pb, Cd and Zn
[b] = Pb, Cd, V, Cr, Co, Ni, Cu, Zn, As and Hg
[c] = Pb, Cd, V, Cr, Mn, Co, Ni, Cu, Zn, As
POPs [d] = α- og γ-HCH, HCB, DDTs, Chlordanes, PCBs, PBDE, HBCD, PAHs, PFAS
[e] = α- og γ-HCH, HCB, PCB
[f] = α- og γ-HCH, HCB, HCHs, DDTs, PCBs, PBDEs, PFAS
[g] = α- og γ-HCH, HCB, DDTs, Chlordanes, PCBs, BDE, HBCDs, PAHs, PFAS, Siloxanes, SCCP, MCCP

Appendix D

Sampling and chemical analysis (incl. background information on PM and EC/OC and levoglucosan)

Main components in precipitation

For precipitation sampling, a NILU Precipitation Collector (funnel + bucket type) is used (P.no. 9713,RS1). The bucket has a size of 2.5 litre, and the diameter of the collecting surface is 200 mm. The collector is placed 2 meters above ground. In winter, during snow conditions, the bulk + funnel collector is exchanged with a so-called Particulate Fallout Collector (P.no. 9711, SF1), see figure on the right of the two bulk collector types. The material used for the collectors is high density polyethylene.

The precipitation sampler is emptied and cleaned with distilled water between each sampling period (daily or weekly), also in periods when there has been no precipitation. The precipitation amount is measured by volume at the site, and an aliquot of the sample is sent to NILU for chemical analysis.

pH is measured with potentiometric method and conductivity with a conductivity meter. Anions and cations are measured with an ion chromatograph. The detection limit for the different ions are given in the table below:

Parameter	Detection limit (unit)
SO_4^{2-}	0.01 (mg S/l)
NO_3^-	0.01 (mg N/l)
NH_4^+	0.01 (mg N/l)
Na^+	0.01 (mg Na/l)
Cl^-	0.01 (mg Cl/l)
K^+	0.01 (mg K/l)
Ca^{2+}	0.01 (mg Ca/l)
Mg^{2+}	0.01 (mg Mg/l)

Main components in air

The main ions in air is sampled with a three stage filterpack using the NILU filter holder system designed for sampling of particles and gaseous compounds, see figure below. The first filter in the air stream is an aerosol filter (Zeflour 2 µm) for collecting the airborne particles containing SO_4^{2-}, NH_4^+, NO_3^-, Ca^{2+}, K^+, Cl^-, Na^+. This is followed by an alkaline (KOH) impregnated filter (Whatman 40), which will collect HNO_3, SO_2, HNO_2, HCl, and other volatile acidic substances. Nitric acid and sulfur dioxide will react with potassium hydroxide on this impregnated filter to give potassium nitrate and potassium sulphite. Oxidizing species in air e.g. ozone are believed to convert most of the sulphite to sulfate during the sampling. The third filter (Whatman 40) is acid-impregnated (oxalic acid) for absorbing alkaline air component such as NH_3. The filter pack method is biased in separating gaseous nitrogen compounds from aerosols and therefore the sum is reported. In other words, the concentration of nitrates in air equals the sum of the nitrate found on the aerosol filter and nitrate found on the alkaline impregnated filter. The same for ammonium, where the sum of ammonium concentration equals the sum of ammonium collected on the aerosol front filter and ammonia collected on the acid impregnated filter.

The filterpack samplers does not have a pre-impactor, but the air intake has a cylindrical vertical plastic section covering the filter holder – about 15 cm wide and 25 cm high. This air intake reduces the sampling efficiency for large particles such as soil dust particles, large sea spray droplets, large pollen,

and fog droplet, thus the size cut off is approximately PM_{10} except for strong sea salt episodes when larger particles are collected.

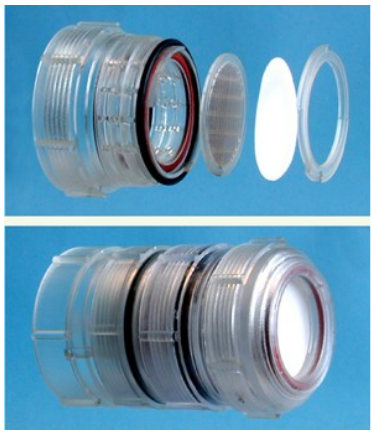

After exposure, the filter holders are sent to NILU for chemical analysis. The filters are put into a test tubes with additions of extraction solution. Hydrogen peroxide solution is used for the alkaline filter in order to oxidize any remaining sulphite to sulfate. An HNO_3 is added to the acid impregnated filter. The aerosol Teflon© filters are given an ultrasonic treatment before analysis in order to obtain a complete extraction. The ions are analysed using an ion chromatograph, and the detection limits are given below:

Parameter	Detection limit (unit)
SO_2	0.01 (µg S/m^3)
SO_4^{2-}	0.01 (µg S/m^3)
Sum (NO_3^-+HNO_3)	0.01 (µg N/m^3)
Sum (NH_4^++NH_3)	0.05-0.1 (µg N/m^3)
Na^+	0.02 (µg Na/m^3)
Cl^-	0.02 (µg Cl/m^3)
K^+	0.02 (µg K/m^3)
Ca^{2+}	0.02 (µg Ca/m^3)
Mg^{2+}	0.02 (µg Mg/m^3)

Nitrogen dioxide

NO_2 is determined with the manual NaI glass sinter method. Ambient air with a flow rate of about 0.5 l/min is drawn through an air intake (inverted funnel) and a glass filter impregnated with sodium iodide (NaI) and sodium hydroxide (NaOH). Nitrogen dioxide is absorbed in the filter, and the iodide reduces NO_2 to nitrite. The nitrite formed on the glass filter is extracted with deionized water. After extraction the nitrite concentration can be determined spectrophotometrically at 540 nm after a reaction with sulphanilamide and N-(1-naphthyl)-ethylenediamine (NEDA). The detection limit for this method is 0.03 µg N/m^3.

Ozone

Ozone (O_3) is determined with the UV-absorption method (UV light at 254 nm) using a monitor with continuous measurements. The results are given in hourly resolution.

Particles (Mass, EC/OC, and levoglucosan)

Background

Size is the most fundamental parameter describing an aerosol, being decisive for transport and removal, and essential for understanding the effects of the ambient aerosol. Aerosol are most commonly defined by their equivalent aerodynamic diameter, defined as, that of a spherical particle of unit density (1 g cm^{-3}), having a settling velocity equal to that of the particle in question. The size distribution of the tropospheric aerosol is commonly divided into three major modes (Whitby, 1978); the nuclei mode, the accumulation mode and the coarse mode, all having different formation processes, leading to different characteristics of the aerosol. Tropospheric aerosols are either emitted directly (primary) or formed in the trophosphere by oxidation of precursor gases (secondary) (Seinfeld and Pandis, 1998). The sources of tropospheric aerosols are both natural (e.g. windborne dust, sea spray, volcanic activity, wild fires) and anthropogenic (fuel combustion, industrial processes, non-industrial fugitive sources and transportation sources), and hence its chemical composition is highly diverse, including amongst others: sulfate (SO_4^{2-}), nitrate (NO_3^-), ammonium (NH_4^+), organic carbon (OC), which is a bulk fraction of numerous organic molecules, light absorbing/refractory carbon (BC/EC), aluminum and silicon (major constituents of mineral dust), inorganic cations (e.g., K^+, Na^+, Ca^{2+} Mg^{2+}) and anions (e.g., Cl^-).

The adverse health effects of the ambient aerosol are well recognized (e.g., Dockery et al., 1993; Schwarz et al., 1996), causing various types of cardiopulmonary diseases, e.g., chronical obstructive pulmonary disease, ischemic heart disease, lung cancer and pneumonia. Although the statistical evidence between ambient air particulate mass (e.g., PM_{10} and $PM_{2.5}$) and adverse health effects are well documented, there is considerable doubt concerning the causal relationship. Thus, other relevant parameters such as the particle number size distribution, the surface and the chemical composition of the aerosol must be considered when addressing this issue. There is strong evidence that fine particles are more hazardous than coarse ones (Schwartz et al., 1996, Schwartz and Neas, 2000), although coarse particles are associated with adverse health effects as well (Castillejos et al., 2000; Ostro et al., 2000). An increasing number of experimental studies have been dedicated to the number of ultrafine particles (d_p< 100 nm), which potentially play a role in the cardiovascular effects commonly associated with exposure to particulate matter (Donaldson et al., 2001). Concerning the chemical composition, WHO has given the general advice that that primary combustion derived particles are particularly important as they "*are often rich in transition metals and organic compounds, and also have a relatively high surface area*". However, more knowledge is needed concerning the ambient aerosol chemical composition and its contribution to the adverse effects seen on human health.

The tropospheric aerosol has an influence on the radiation budget both directly, by scattering and absorption of sunlight and terrestrial radiation, and indirectly, by influencing cloud reflectivity and lifetime. Both effects lead to a mostly cooling effect for the Earth's surface. The particle size distribution is essential for quantifying the magnitude of both direct and indirect aerosol climate effect, whereas particle chemical composition influences aerosol absorption and the lower size limit of particles acting as cloud condensation nuclei.

The tropospheric aerosol also plays an important role when it comes to acidification and eutrophication of water bodies. This is attributed to the content of secondary inorganic species such as SO_4^{2-}, NO_3^- and NH_4^+, which typically are associated with accumulation mode particles, enabling long-range transport and deposition in regions far from where the precursors where emitted.

Elemental (EC) and organic (OC) carbon are important fractions of the ambient aerosol particle, contributing to the aerosol particle influence on the radiation budget both directly, by scattering and

absorption of sunlight, and indirectly, by cloud formation. Likewise does the carbonaceous fraction contribute to the adverse health effects observed, i.e., respiratory and cardiovascular diseases. EC enters the atmosphere exclusively as a primary (i.e., direct particulate) emission, whereas OC includes both primary aerosol particles and secondary aerosol particles, of which the latter is formed from gaseous precursors oxidized in the atmosphere. The carbonaceous fraction can be of both anthropogenic and natural origin, e.g., EC and OC from incomplete combustion of fossil fuel (e.g., vehicular tailpipe emissions) and biomass (residential wood burning and wildfires), OC from oxidation of gaseous emissions from coniferous and deciduous trees, and OC associated with primary biological aerosol particles (PBAP). EC and OC are typically associated with the fine aerosol particle, although OC can appear in the coarse fraction as well, e.g., the PBAPs or due to condensation of OC on coarse aerosol particles. Despite the importance of the carbonaceous aerosol, detailed apportionment and quantification of its sources is still difficult due to the large number of sources, the complexity of atmospheric formation and the vast number of organic compounds associated with the aerosol.

EC and OC are simply operational definitions, and do not provide information about the source *pr. se*, thus additional measurements to EC and OC are required to provide information about the carbonaceous aerosol sources and their relative share. Source apportionment studies (Yttri et al., 2011a, b; Yttri et al.., 2021) including both ^{14}C and organic tracers show that natural sources dominate OC in PM_{10} at Norwegian rural background sites in summer, of which OC associated with the biogenic secondary organic aerosol (BSOA) is the major source followed by OC associated with PBAP. In winter, anthropogenic sources dominates OC in PM_{10}, i.e., emissions from fossil fuel combustion and residential wood burning. The picture is rather similar for OC in PM_1, except that OC associated with PBAP is of much less importance in summer than seen for PM_{10}. Combustion of fossil fuel appears to be the major source of EC regardless of season and size fraction, but EC from residential wood burning increases substantially in winter.

Levoglucosan is a thermal degradation product of cellulose with a low vapor pressure and a high emission factor from combustion of biomass (Locker, 1988; Simoneit et al., 1999; Oja and Suuberg, 1999), and thus well suited to trace biomass-burning aerosol in the ambient atmosphere. Aqueous-phase reaction with OH radical in deliquescent particles appears to be the most efficient pathway causing depletion of levoglucosan in the atmosphere. The ½ values (the time until half of the levoglucosan has been degraded) for levoglucosan in the atmosphere is debated and likely to vary with photochemical activity and OH concentrations, being a function of temperature and season (Hennigan et al., 2010; Yttri et al., 2014).

Levoglucosan is considered the most robust and reliable tracer of biomass burning, and is commonly used to trace biomass burning aerosol, not only qualitatively, but also quantitatively by combining ambient concentrations with emission ratios, or as input along with other species to e.g. positive matrix factorization (PMF). For studies using levoglucosan as biomass burning tracer in Norway, see Yttri et al., 2005, 2007a, b, 2009, 2011a, b, 2014, 2021, 2023 (Subm.). Although levoglucosan appears to be best suited to trace biomass burning emissions in winter and on a local to regional scale, conservative estimates of the biomass burning aerosol concentration can still be provided for the remote environment. Emission ratios used to convert observed ambient concentrations of levoglucosan to OC and EC from biomass burning, are associated with great uncertainty. In the present report, we use an OC/levoglucosan ratio of 12.7 for PM_{10} and 11.1 for $PM_{2.5}$ and an EC/levoglucosan ratio of 2. These ratios are based on positive matrix factorization (PMF) analysis results for PM and PM species observed at Birkenes (Yttri et al., 2021), which are consistent with results presented in the scientific literature e.g., by Zotter et al. (2017). A factor of 2 was used to convert biomass burning OC to OM, and a factor of 1.1 for biomass burning EC.

Sampling and chemical analysis

PM_{10} and $PM_{2.5}$ are obtained using Kleinfiltergerät samplers (one sampler pr. size faction), collecting filter samples on a weekly basis. The ambient aerosol particles are collected on prefired (850 °C; 3 h) quartz fibre filters (Whatman QM-A, 47 mm). The quartz fibre filters are conditioned (20 °C; 50% RH; 48 h) prior to and after being exposed. The mass concentration of the quartz fibre filters is determined gravimetrically. The uncertainty of the PM mass concentrations obtained for PM_{10} and $PM_{2.5}$ is estimated to be around 0.1 – 0.15 µg/m^3 for a sampling volume of 386 m^3.

Number concentration measurements at Birkenes dates back to 2010. The number concentration of ultrafine particles (D_p <0.1 µm), accumulation mode particles (0.1 µm < D_p < 1.0 µm) and coarse mode particles (D_p = 1.0 - 10 µm) are obtained by combined measurements of a Differential Mobility Particle Spectrometer (DMPS) and an Optical Particle Spectrometer (OPS). The DMPS measures the particle number size distribution ranging from 0.01 – 0.8 µm particle diameter, whereas the OPS covers the range from 0.25 µm to 30 µm. The DMPS and the OPS provide method specific measures of the particle diameter, i.e., the electrical mobility particle diameter and the optical particle diameter, respectively. Thus, when merging these two measures into one particle number size distribution (PNSD) time series, the PNSD must agree within 25% in particle diameter in their overlapping size range. For comparability of long-term measurements, the 0.01 – 0.02 µm size range is not reported.

In May 2017, a continuous, direct aerosol mass instrument was installed at Birkenes, a so-called tapered element oscillating microbalance (TEOM) instrument with a size cut off to measure PM_{10} mass. The TEOM Monitor draws (then heats) ambient air through a filter at constant flow rate, continuously weighing the filter and calculating near real-time mass concentrations of particulate matter. The mass is corrected with a factor 1.1 and -2.8 µg m^{-3} based on intercomparison with gravimetric measurements, which is the reference method.

Thermal-Optical Analysis of EC, OC and TC in PM_{10} and $PM_{2.5}$ are performed on the same filter samples as the mass concentration of PM_{10} and $PM_{2.5}$ are obtained from at the three rural background sites. For the remote site Zeppelin, analysis is performed on prefired (850 °C; 3 hrs) quartz fibre filters (PALLFLEX Tissuequartz 2500QAT-UP; 150 mm in diameter) obtained from a Digitel high-volume sampler with a PM_{10} inlet, operating at a flowrate of 40 m^3 h^{-1}, collecting aerosol filter samples on a weekly basis. The T-O analysis are performed according to the EUSAAR-2 protocol (Cavalli *et al.*, 2010). The analytical detection limit of the TOA instruments is 0.2 µg C/cm^2. This corresponds to a methodological detection limit of 0.007 µg C m^{-3} for a sampling volume of 386 m^3 and an exposed filter area of 13.4 cm^2 for the rural background sites and, and a methodological detection limit of 0.005 µg C m^{-3} for a sampling volume of 6720 m^3 and an exposed filter area of 153.9 cm^2 for the remote site.

Concentrations of the biomass burning tracers levoglucosan, mannosan and galactosan are determined from the same PM_{10} filter samples as the mass concentration, OC, EC and TC at the rural background sites and from the same PM_{10} filter samples as OC, EC and TC at the remote site. Analysis is performed using ultra-high performance liquid chromatography (UHPLC) in combination with high-resolution time-of-flight mass spectrometry (HR-TOF-MS) operated in the negative electrospray ionization (ESI-) mode, and according to a modified version of the analytical method described by Dye and Yttri (2005) (Yttri et al., 2021). The methodological detection limit is approximately 1-20 pg m^{-3} for the rural background sites and 1-4 pg m^{-3} for the remote site.

References:

Dye, C., Yttri, K.E. (2005) Determination of monosaccharide anhydrides in atmospheric aerosols by use of high-resolution mass spectrometry combined with high performance liquid chromatography. *Anal. Chem., 77,* 1853-1858.

Hennigan, C. J., Sullivan, A. P., Collett Jr., J. L., and Robinson, A. L. (2010) Levoglucosan stability in biomass burning particles exposed to hydroxyl radicals. *Geophys. Res. Lett., 37,* L09806, doi:10.1029/2010GL043088.

Locker, H.B. (1998) PhD Dissertation, Dartmouth College, Hanover, NH.

Oja, V. and Suuberg, E. M. (1999) Vapor Pressures and Enthalpies of Sublimation of D-glucose, D-xylose, Cellobiose, and Levoglucosan. *J. Chem. Eng. Data, 33,* 26–29.

Simoneit, B. R. T., Schauer, J. J., Nolte, C. G., Oros, D. R., Elias, V.O., Fraser, M. P., Rogge,W. F. and Cass., G. R. (1999) Levoglucosan, a tracer for cellulose in biomass burning and atmospheric particles. *Atmos. Environ., 33, 173–182*.

P. Zotter, V. G. Ciobanu, Y. L. Zhang, I. El-Haddad, M. Macchia, K. R. Daellenbach, G. A. Salazar, R.-J. Huang, L. Wacker, C. Hueglin7, A. Piazzalunga, P. Fermo, M. Schwikowski, U. Baltensperger, S. Szidat and A. S. H. Prévôt (2014) Radiocarbon analysis of elemental and organic carbon in Switzerland during winter-smog episodes from 2008 to 2012 – Part 1: Source apportionment and spatial variability. *Atmos. Chem. Phys., 14,* 13551–13570. doi:10.5194/acp-14-13551-2014.

Yttri, K. E., Dye, C., Slørdal, L. H. and Braathen, O.-A. (2005) Quantificationof monosaccharide anhydrides by negative electrospray HPLC/HRMS-TOF – Application to aerosol samples from an urban and a suburban site influenced by small scale wood burning. *J. Air Waste Manage. Assoc., 55,* 1169–1177.

Yttri, K.E., Dye, C. and Kiss, G. (2007a) Ambient aerosol concentrations of sugars and sugar-alcohols at four different sites in Norway. *Atmos. Chem. Phys., 7,* 4267-4279. doi:10.5194/acp-7-4267-2007.

Yttri, K.E., Aas, W., Bjerke, A., Cape, J.N., Cavalli, F., Ceburnis, D., Dye, C., Emblico, L., Facchini, M.C., Forster, C., Hanssen, J.E., Hansson, H.C., Jennings, S.G., Maenhaut, W., Putaud, J.P. and Tørseth, K. (2007b) Elemental and organic carbon in PM_{10}: a one year measurement campaign within the European Monitoring and Evaluation Programme EMEP. *Atmos. Chem. Phys., 7,* 5711–5725, doi:10.5194/acp-7-5711-2007.

Yttri, K. E., Dye, C., Braathen, O.-A., Simpson, D. and Steinnes, E. (2009) Carbonaceous aerosols in Norwegian urban sites. *Atmos. Chem. Phys., 9,* 2007–2020, doi:10.5194/acp-9-2007-2009.

Yttri, K.E., Simpson, D., Stenström, K., Puxbaum, H. and Svendby, T. (2011a) Source apportionment of the carbonaceous aerosol in Norway - quantitative estimates based on 14C, thermal-optical and organic tracer analysis. *Atmos. Chem. Phys., 11,* 9375-9394. doi:10.5194/acp-11-9375-2011.

Yttri, K.E., Simpson, D., Nøjgaard, J.K., Kristensen, K., Genberg, J., Stenström, K., Swietlicki, E., Hillamo, R., Aurela, M., Bauer, H., Offenberg, J.H., Jaoui, M., Dye, C., Eckhardt, S., Burkhart, J.F., Stohl, A. and Glasius, M. (2011b) Source apportionment of the summer time carbonaceous aerosol at Nordic rural background sites. *Atmos. Chem. Phys., 11,* 13339-13357. doi:10.5194/acp-11-13339-2011.

Yttri, K.E., Myhre, C.L., Eckhardt, S., Fiebig, M., Dye, C., Hirdman, D., Ström, J., Klimont, Z. and Stohl, A. (2014) Quantifying black carbon from biomass burning by means of levoglucosan – a one-year time series at the Arctic observatory Zeppelin. *Atmos. Chem. Phys., 14,* 6427-6442. doi:10.5194/acp-14-6427-2014.

Yttri, K. E., Canonaco, F., Eckhardt, S., Evangeliou, N., Fiebig, M., Gundersen, H., Hjellbrekke, A.-G., Lund Myhre, C., Platt, S. M., Prévôt, A. S. H., Simpson, D., Solberg, S., Surratt, J., Tørseth, K., Uggerud, H., Vadset, M., Wan, X., and Aas, W. (2021) Trends, composition, and sources of carbonaceous aerosol at the Birkenes Observatory, northern Europe, 2001–2018. *Atmos. Chem. Phys., 21*, 7149–7170. doi:10.5194/acp-21-7149-2021.

Yttri, K. E., Bäcklund, A., Conen, F., Eckhardt, S., Evangeliou, N., Fiebig, M., Kasper-Giebl, A., Gold, A., Gundersen, H., Myhre, C. L., Platt, S. M., Simpson, D., Surratt, J. D., Szidat, S., Rauber, M., Tørseth, K., Ytre-Eide, M. A., Zhang, Z., and Aas, W.: Composition and sources of carbonaceous aerosol in the European Arctic at Zeppelin Observatory, Svalbard, EGUsphere [preprint], https://doi.org/10.5194/egusphere-2023-615, 2023.

NILU – Norwegian Institute for Air Research

NILU – Norwegian Institute for Air Research is an independent, non-profit institution established in 1969. Through its research NILU increases the understanding of climate change, of the composition of the atmosphere, of air quality and of hazardous substances. Based on its research, NILU markets integrated services and products within analysing, monitoring and consulting. NILU is concerned with increasing public awareness about climate change and environmental pollution.

NILU's values: *Integrity - Competence - Benefit to society*
NILU's vision: *Research for a clean atmosphere*

NILU – Norwegian Institute for Air Research
P.O. Box 100, NO-2027 KJELLER, Norway

E-mail: nilu@nilu.no
http://www.nilu.no

ISBN: 978-82-425-3122-3
ISSN: 2464-3327

Norsk institutt for luftforskning
Norwegian Institute for Air Research